


Synchronization effects on rest frame energy and momentum densities in the proton

Adam Freese^{1,2,*} and Gerald A. Miller^{2,†}¹Theory Center, Jefferson Lab, Newport News, Virginia 23606, USA²Department of Physics, University of Washington, Seattle, Washington 98195, USA
 (Received 8 August 2023; revised 18 October 2023; accepted 31 October 2023; published 16 November 2023)

We obtain two-dimensional relativistic densities and currents of energy and momentum in a proton at rest. These densities are obtained at surfaces of fixed light front time, which physically corresponds to using an alternative synchronization convention. Mathematically, this is done using tilted light front coordinates, which consist of light front time and ordinary spatial coordinates. In this coordinate system, all 16 components of the energy-momentum tensor (EMT) obtain clear physical interpretations, and the nine Galilean components reproduce results from standard light front coordinates. We find angular modulations in several densities that are absent in the corresponding instant form results, which are explained as optical effects arising from using fixed light front time when motion is present within the target. Additionally, transversely polarized spin-half targets exhibit an energy dipole moment—which evaluates to $-1/4$ for all targets if the Belinfante EMT is used, but which is target dependent and vanishes for pointlike fermions if the asymmetric EMT is instead used.

DOI: 10.1103/PhysRevD.108.094026

I. INTRODUCTION

Significant attention has been placed on the energy-momentum tensor (EMT) and the associated gravitational form factors [1] over the past few years. Major questions in the field of hadron physics, such as the proton mass puzzle [2–8] and proton spin puzzle [9–13] are directly related to the EMT. Additionally, there has been much discussion over how (and whether) the EMT encodes distributions of static forces within hadrons [8,14–18]. This attention is especially pertinent with the anticipated construction of the Electron Ion Collider [19–21], since the measurement of generalized parton distributions [22–24] is the most promising means of empirically accessing the gravitational form factors.

Currently the literature is filled with a variety of perspectives on how to obtain spatial distributions of local currents in composite systems, including those encoded by the EMT (see, for instance, Refs. [15,16,25–35]). The light front formalism stands out among these as providing relativistically exact two-dimensional (2D) densities [36,37] that are obtained from elementary

field-theoretic definitions [17,26] in a wave-packet-independent way [31]. Misgivings have been expressed about the light front densities with the understanding that they constitute a description of the system moving at infinite momentum [38]. However, in a recent work [33], we showed that light front densities constitute *rest frame densities* within hadrons at a fixed light front time by utilizing a coordinate system called tilted light front coordinates (or tilted coordinates):

$$\tau = x^0 \equiv t_{\text{IF}} + z_{\text{IF}}, \quad (1a)$$

$$x = x^1 \equiv x_{\text{IF}}, \quad (1b)$$

$$y = x^2 \equiv y_{\text{IF}}, \quad (1c)$$

$$z = x^3 \equiv z_{\text{IF}}, \quad (1d)$$

first proposed by Blunden, Burkardt, and Miller [39]. By using light front time τ but ordinary Cartesian spatial coordinates (x, y, z) , the Galilean subgroup of the Poincaré group can be exploited while utilizing everyday intuition about space, including that a target is at rest when $(v_x, v_y, v_z) = (0, 0, 0)$.

Operationally, the use of tilted coordinates corresponds to synchronizing spatially distant clocks under the assumption that the speed of light is infinite in the $-z$ direction, and consequently the light front densities constitute a literal picture of what an observer looking in the $+z$ direction sees when their local time is τ . In our prior

*afreese@jlab.org

†miller@uw.edu

Published by the American Physical Society under the terms of the [Creative Commons Attribution 4.0 International license](https://creativecommons.org/licenses/by/4.0/). Further distribution of this work must maintain attribution to the author(s) and the published article's title, journal citation, and DOI. Funded by SCOAP³.

work [33] we refer to this synchronization rule as *light front synchronization*. Light front synchronization stands in contrast to the standard Einstein synchronization convention [40], under which spatially distant clocks are synchronized by assuming that the one-way speed of light is isotropic and equal to c in all directions. Using Einstein synchronization results in the standard Minkowski (or instant form) coordinate system, in which the observer is understood to see a past state of the system they are observing. (See Refs. [41–45] for detailed discussions of synchronization conventions.)

Previously, we obtained the rest frame electromagnetic currents of the proton and neutron in tilted light front coordinates [33]. The purpose of the present work is to obtain the energy and momentum currents encoded by the EMT within the same formalism. A variety of EMT densities already exist in the literature in different formalisms, but the tilted coordinate framework offers a number of advantages that make the presentation of new EMT densities worthwhile. Much like the standard light front densities, the densities obtained in tilted coordinates are relativistically exact, while the more commonly used Breit frame densities are leading-order contributions that dominate for spatially diffuse wave packets [29,31], and are as such subject to relativistic corrections [15]. Moreover, when localizing wave packets in instant form coordinates, the resulting densities differ from the Breit frame densities [32,35,46], since the dominating term in an infinite series differs for localized wave packets [29]. The standard light front and tilted light front densities, by contrast, are fully independent of the target's wave packet [31,33].

There are also several advantages to using tilted light front coordinates over standard light front coordinates when obtaining densities. One of these is the ability to clearly show that the results are rest frame densities. Additionally, for local currents such as the electromagnetic current $j^\mu(x)$ and the energy-momentum tensor $T^{\mu\nu}(x)$, every component of the current obtains a clear physical interpretation in tilted coordinates. By contrast, the components $j^-(x)$, $T^{i-}(x)$, and $T^{-i}(x)$ do not have clear

interpretations in standard light front coordinates, and accordingly are typically ignored. In this work, we will present results for all 16 components of the proton's EMT density.

One last benefit of tilted coordinates over standard light front coordinates is that the tilted energy E is exactly equal to the standard instant form energy, and that the tilted energy density

$$\begin{aligned} \mathcal{E}(\mathbf{b}_\perp, \hat{s}) = m \int \frac{d^2\Delta_\perp}{(2\pi)^2} & \left(A(-\Delta_\perp^2) + \frac{\Delta_\perp^2}{4m^2} D(-\Delta_\perp^2) \right. \\ & + \frac{(\hat{s} \times \mathbf{i}\Delta_\perp) \cdot \hat{e}_z}{2m} \left\{ B(-\Delta_\perp^2) - J(-\Delta_\perp^2) \right. \\ & \left. \left. - \frac{\Delta_\perp^2}{4m^2} D(-\Delta_\perp^2) \right\} \right) e^{-i\Delta_\perp \cdot \mathbf{b}_\perp} \end{aligned} \quad (2)$$

is thus an exact 2D relativistic distribution of the usual energy E , rather than of P^- . The tilted energy density is thus more pertinent to debates about the proton mass decomposition, which typically frame the mass decomposition as an energy decomposition [2–4,6–8]. [Equation (2) will be proved below in Sec. V after the necessary formalism has been developed. Table I can be consulted to quickly find explicit results to the EMT densities, as well as their analogs in standard light front coordinates and the Breit frame formalism.]

Tilted coordinates have several unfamiliar mathematical properties, and this work is not intended as an introduction to them. We have compiled a collection of helpful basic properties and identities in Appendix A for easy access, but a full exposition of the coordinate system is given in Ref. [33]. The remainder of this work uses tilted coordinates and contains occasional reminders of their idiosyncratic properties.

This work is organized as follows. In Sec. II, we explain how components of the energy-momentum tensor are interpreted as furnishing densities and flux densities of energy and momentum, and provide a dictionary for converting components of the EMT into energy and

TABLE I. Explicit results for EMT densities of spin-half targets in the Breit frame formalism, in the standard light frame formalism, and in tilted coordinates can be found in the references and equations provided in this table. The references have been chosen for easy consultation and for providing formulas for arbitrary polarization, rather than for original discovery. In several cases, standard light front results do not exist, or only exist for transverse components. Reference [16] provides a light front P^- density in its Eq. (107), but is excluded from the table because $P^- \neq E$ and because the result is only for unpolarized targets. In several other cases, standard light front densities are obtainable, but we could not find results for them in the literature, so we have pointed to equivalent formulas in the present work.

| Component | Breit frame | Standard light front | Tilted coordinates |
|---------------------|---|---|--------------------|
| Energy density | $T^0_0(\mathbf{x})$ Eq. (17a) of [15] | ... | Eq. (2) |
| Momentum density | $-T^0_i(\mathbf{x})$ Eq. (17c) of [15] | Eqs. (11) and (20) of Ref. [47] [long.] Same as Eq. (38b) [trans.] | Eq. (38) |
| Energy flux density | $T^i_0(\mathbf{x})$ Same as Eq. (17c) of [15] | Same as Eq. (42) [trans. only] | Eq. (42) |
| Stress tensor | $-T^i_j(\mathbf{x})$ Eq. (17b) of [15] | Eq. (21) of [47] [trans. only] | Eq. (43) |

momentum currents. In Sec. III, we explore how expectation values of the EMT for physical states can be decomposed into internal rest frame distributions and state-dependent smearing functions, the latter of which absorbs dependencies on the target's overall motion. Next, in Sec. IV, we obtain the rest frame energy and momentum currents for a spin-zero target as a warm-up exercise. Section V then provides expressions for the rest frame EMT densities of a spin-half target as well as numerical examples for a proton. Finally, we conclude in Sec. VI.

Throughout this work—and in contrast to our previous work on the subject [33]—we do not include any special markings (such as a tilde) to indicate that tilted coordinates are being used. Unless explicitly indicated otherwise (such as by a subscript or superscript IF for “instant form”), all noninvariant quantities should be assumed to signify a quantity in tilted coordinates.

II. ENERGY AND MOMENTUM CURRENTS IN TILTED COORDINATES

The EMT is a local operator characterizing the distribution and flow of energy and momentum of a system. In quantum chromodynamics (QCD), the operator is formally given by [11,48]

$$\hat{T}_{\text{QCD}}^{\mu\nu} = \sum_q \frac{i}{4} \bar{q} \gamma^{\{\mu} \overleftrightarrow{D}^{\nu\}} q + F_a^{\mu\rho} F_\rho^{a\nu} - A_a^{\{\mu} (\partial^{\nu\}} B_a) - i(D^{\{\mu} c)(\partial^{\nu\}} \bar{c}) - g^{\mu\nu} \mathcal{L}_{\text{QCD}}, \quad (3)$$

where \mathcal{L}_{QCD} is the QCD Lagrangian

$$\mathcal{L}_{\text{QCD}} = \sum_q \bar{q} \left(\frac{i}{2} \overleftrightarrow{\partial} + g \mathcal{A}_a T^a - m_q \right) q - \frac{1}{4} F_{\mu\nu}^a F_a^{\mu\nu} - (\partial_\mu B_a) A_a^\mu + \frac{\alpha_0}{2} B_a^2 - i(\partial_\mu \bar{c}^a)(D_{ab}^\mu c^b). \quad (4)$$

Here A_a^μ is the gluon four-potential, B_a are Lagrange multiplier fields, and c_a and \bar{c}_a are the Faddeev-Popov ghosts. The Lagrange multiplier and ghost fields are unphysical and annihilate physical states, but are necessary to quantize and renormalize the theory [48]. The different representations of the gauge-covariant derivative are

$$\overrightarrow{D}_\mu q = \overrightarrow{\partial}_\mu q - ig A_\mu^a T_a q, \quad (5a)$$

$$\overleftarrow{D}_\mu \bar{q} = \overleftarrow{\partial}_\mu \bar{q} + ig \bar{q} A_\mu^a T_a, \quad (5b)$$

$$D_\mu^{ab} c^b = (\delta_{ab} \partial_\mu + gf_{acb} A_\mu^c) c^b, \quad (5c)$$

and the gluon field strength tensor is

$$F_{\mu\nu}^a = \partial_\mu A_\nu^a - \partial_\nu A_\mu^a + gf_{abc} A_\mu^b A_\nu^c. \quad (6)$$

Here, T_a are the generators of the color $\mathfrak{su}(3, \mathbb{C})$ algebra and f_{abc} are the totally antisymmetric structure constants defined by

$$[T_a, T_b] = if_{abc} T_c. \quad (7)$$

The EMT can be derived through several methods. Noether's first theorem and invariance of the QCD action under global spacetime translations infamously results in an EMT that is not gauge invariant [11,24,48], but this is rectified through the Belinfante improvement procedure [49], which adds a trivially conserved quantity to the EMT in order to restore gauge invariance. The trivially conserved quantity is usually chosen to reproduce Eq. (3). However, Leader and Lorcé [11] show that an alternative EMT can be obtained, with an additional antisymmetric piece $\hat{T}_A^{\mu\nu}(x)$:

$$\begin{aligned} \hat{T}_{\text{asym}}^{\mu\nu}(x) &= \hat{T}_{\text{QCD}}^{\mu\nu}(x) + \sum_q \left\{ \frac{1}{2} \bar{q}(x) \gamma^{\{\mu} i \overleftrightarrow{D}^{\nu\}} q(x) \right\} \\ &\equiv \hat{T}_{\text{QCD}}^{\mu\nu}(x) + \hat{T}_A^{\mu\nu}(x). \end{aligned} \quad (8)$$

The antisymmetric piece is interpreted as describing intrinsic fermion spin; see Ref. [11] for further details.

The EMT can alternatively be derived using Noether's second theorem while assuming invariance of the QCD action under local spacetime translations [50]. If fermion fields transform according to their Lie derivative under these local translations, the resulting EMT is exactly that in Eq. (3). The EMT in Eq. (3) can also be obtained by taking the functional derivative of the QCD action with respect to the metric tensor [24] or with respect to the vierbein [48]. These methods avoid the need for an improvement procedure to ensure gauge invariance and lack an ambiguity about the resulting EMT.

Regardless of whether the antisymmetric piece $\hat{T}_A^{\mu\nu}(x)$ is included in the EMT, integrals of the EMT over equal-time surfaces reproduce the generators of spacetime translations, as a consequence of being the conserved Noether current associated with spacetime translation symmetry. If V is a fixed-time hypersurface and n_μ is a unit forward-directed normal to this surface:

$$\hat{P}^\nu(\tau) = \int_V d^3 \mathbf{x} n_\mu \hat{T}^{\mu\nu}(x, \tau), \quad (9)$$

where τ is the time variable under consideration. If instant form time (the time resulting from Einstein synchronization) is used to define equal-time surfaces, then n_μ is a timelike vector pointing in the forward- t_{IF} direction. If light front time $t_{\text{IF}} + z$ is instead used to define equal-time surfaces, n_μ is a lightlike vector pointing along the light cone. The latter scenario is depicted with a finite hypersurface in Fig. 1. If V is extended to all of space, then \hat{P}^ν

is conserved, and thus time-independent, by virtue of Noether's theorems.

The four-vector operator \hat{P}_ν plays the role of a spacetime translation generator, specifically in its covariant form (with a lower index):

$$i[\hat{P}_\nu, \hat{O}(x)] = \partial_\nu \hat{O}(x). \quad (10)$$

The contravariant (upper-index) components of the four-momenta are related to the covariant components through $\hat{P}^\nu = g^{\nu\rho} \hat{P}_\rho$. In instant form coordinates, this gives a trivial relationship for components of the vector momentum:

$$\hat{P}_{\text{IF}} = (\hat{P}_{\text{IF}}^1, \hat{P}_{\text{IF}}^2, \hat{P}_{\text{IF}}^3) = (-\hat{P}_1^{(\text{IF})}, -\hat{P}_2^{(\text{IF})}, -\hat{P}_3^{(\text{IF})}), \quad (11)$$

but in tilted coordinates the relationship is more complicated—see Eq. (A2) for the metric tensor in tilted coordinates and Eq. (A3) for the covariant-contravariant relations. To play their proper role as space translation generators, components of vector momentum are identified through *covariant* components of the four-momentum: $\hat{P} = (-\hat{P}_1, -\hat{P}_2, -\hat{P}_3)$. Likewise, the Hamiltonian (as the time translation generator) is given by \hat{P}_0 . Accordingly, the energy and momentum densities are associated with the mixed upper-lower form of the EMT, $\hat{T}^\mu{}_\nu(x)$, which can be interpreted as a \hat{P}_ν current. As such, $\hat{T}^\mu{}_0(x)$ gives an energy-four current—a combination of an energy density and energy flux density—while $-\hat{T}^\mu{}_i(x)$ encodes three vector momentum currents.

As is standard in continuum mechanics [51–56], flux densities of momentum can be interpreted as stresses. We review the rationale behind this. By virtue of Noether's theorems, the EMT obeys a continuity equation,

$$\partial_\mu T^\mu{}_\nu(x) = 0, \quad (12)$$

which is the differential form of energy-momentum conservation. If we integrate this differential form over the spacetime region Ω depicted in Fig. 1 and use the divergence theorem, we obtain the integral form of the conservation law

$$\frac{d}{d\tau} [T^0{}_\nu(x, \tau)] = - \oint_{\partial V} dA_i T^i{}_\nu(x, \tau), \quad (13)$$

where ∂V is the boundary of the spatial region V and dA is an area element with outward-pointing normal. This equation describes the amount of P_ν in a spatial region V changing due to the flux of P_ν through the boundary of this region. For this reason, $T^0{}_\nu(x, \tau)$ is the P_ν density and $T^i{}_\nu(x, \tau)$ is the P_ν flux density. For $\nu \in \{1, 2, 3\}$ this equation describes a net change of momentum in the region:

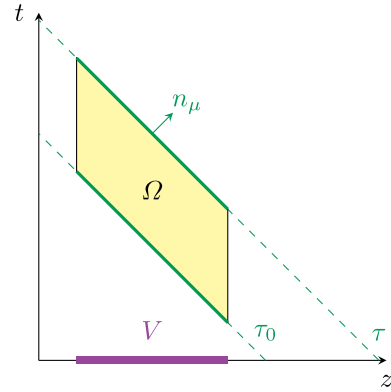


FIG. 1. A finite spacetime region Ω bounded by two hypersurfaces of equal light front time τ_0 and τ , drawn in terms of instant form coordinates. Each slice of fixed light front time contains the same spatial region V . The future-directed normal n_μ to the equal-light-front-time hypersurfaces is also indicated in this diagram.

$$\mathbf{F}_V(\tau) \equiv - \frac{d}{d\tau} [\mathbf{P}_V(\tau)] = - \hat{e}_j \oint_{\partial V} dA_i T^i{}_j(\mathbf{x}, \tau). \quad (14)$$

Since momentum is leaving (or entering) the region V , this will be felt by the region's surroundings as a force $\mathbf{F}_V(\tau)$, exerted by the region, which would be measured, for instance, by a hypothetical pressure gauge placed at the boundary ∂V . Accordingly, $-\hat{e}_j T^i{}_j(\mathbf{x}, \tau)$ is a force per unit area on a surface with a unit normal \hat{e}_i , and thus has a straightforward interpretation as a pressure. More generally, $-T^i{}_j(\mathbf{x}, \tau)$ is referred to as the stress tensor and encodes the pressures that would be measured on a surface in any orientation.

For a system in equilibrium, one will have zero net force exerted by any region V , and thus equal fluxes of momentum into and out of any region. In integral form, the equilibrium condition is

$$\hat{e}_j \oint_{\partial V} dA_i T^i{}_j(\mathbf{x}, \tau) = 0, \quad (15)$$

but the divergence theorem can be used to require this in differential form:

$$\partial_i T^i{}_j(\mathbf{x}, \tau) = 0. \quad (16)$$

This is possible even when $T^i{}_j(\mathbf{x}, \tau) \neq 0$. If the stress tensor is nonzero in an equilibrium system, this means that static pressures will be felt, and in general the pressures will be anisotropic. The components of $S^{ij}(\mathbf{x}, \tau) \equiv -T^i{}_j(\mathbf{x}, \tau)$ are referred to as stresses and $S^{ij}(\mathbf{x}, \tau)$ itself as the stress tensor, and these have an interpretation as furnishing mechanical pressures in a variety of continuum systems [51,53,55,56], including fluids [52], solids [57], liquid crystals [58–60], and neutron stars [54,61]. (See also Ref. [62] for a unified

treatment of liquids, crystals, and liquid crystals.) Since the fundamental ontological objects of quantum field theory are fields rather than particles, it is sensible to interpret QCD as a theory of a continuous medium as well, and to interpret components of the operator $-\hat{T}^i_j(x)$ as stresses in this medium.

Although the mixed upper-lower form of the EMT has the most straightforward interpretation in terms of energy-momentum four-currents, it is convenient to work with tensors having all upper indices. The rules for raising and lowering indices in Eq. (A3) can be used to rewrite the energy-momentum four-currents entirely in terms of $T^{\mu\nu}(x)$. In light of this, the following dictionary can be quickly consulted to ascribe physical meanings to components of the EMT in tilted coordinates:

(i) *Energy density*:

$$\mathcal{E}(x) = T^0_0(x) = T^{00}(x) - T^{03}(x). \quad (17a)$$

(ii) *Energy flux density*:

$$\mathcal{F}_E(x) = T^i_0(x)\hat{e}_i = (T^{i0}(x) - T^{i3}(x))\hat{e}_i. \quad (17b)$$

(iii) *Momentum density*:

$$\begin{aligned} \mathcal{P}(x) &= -T^0_i(x)\hat{e}_i \\ &= T^{01}(x)\hat{e}_x + T^{02}(x)\hat{e}_y + T^{00}(x)\hat{e}_z. \end{aligned} \quad (17c)$$

(iv) *Stress tensor* (i.e., momentum flux densities):

$$\begin{aligned} S^{ij}(x) &= -T^i_j(x) \\ &= T^{i1}(x)\delta^{j1} + T^{i2}(x)\delta^{j2} + T^{i0}(x)\delta^{j3}. \end{aligned} \quad (17d)$$

III. CONVOLUTION FORMALISM FOR PHYSICAL CURRENTS

In our previous work [31,33], we suggested that physical relativistic densities be identified as expectation values of local currents for physical states, which include information about how the system is prepared (in particular, its wave packet). If a physical state is described by a density matrix $\hat{\rho}$ (which is equal to $|\Psi\rangle\langle\Psi|$ for a pure state), this expectation value can be written (in the Heisenberg picture):

$$\langle J^\mu(x) \rangle = \text{Tr}[\hat{\rho}\hat{J}^\mu(x)] \xrightarrow{\text{pure state}} \langle\Psi|\hat{J}^\mu(x)|\Psi\rangle. \quad (18)$$

The central idea of Ref. [33] is that if the density is considered at fixed *light front time* τ rather than fixed Minkowski time, and if the longitudinal coordinate is integrated out, then the physical density can be factorized into a piece that depends only on its intrinsic structure and a

universal smearing function, the latter of which absorbs all wave-packet dependence. In particular,¹

$$\begin{aligned} \langle J^\mu(\mathbf{x}_\perp, \tau) \rangle_{2D} &\equiv \int d^3x \langle J^\mu(x) \rangle \\ &= \sum_{\lambda, \lambda'} \int d^2\mathbf{R}_\perp \mathcal{P}^\mu_\nu(\mathbf{R}_\perp, \tau; \lambda, \lambda') \\ &\quad \times j^\nu(\mathbf{x}_\perp - \mathbf{R}_\perp; \lambda, \lambda'), \end{aligned} \quad (19)$$

where j^ν is the intrinsic four-current density and \mathcal{P}^μ_ν is the smearing function. The intrinsic density retains no information about the system's wave packet, encoding only information about its internal structure (which will differ between different hadron species), while the smearing function is independent of hadron species and absorbs all wave-packet dependence. The very possibility of this factorization requires the use of light front synchronization, as proved in Appendix B of Ref. [33].

This relation should generalize to the energy-momentum tensor,

$$\begin{aligned} \langle T^{\mu\nu}(\mathbf{x}_\perp, \tau) \rangle_{2D} &= \int d^3x \text{Tr}[\hat{\rho}\hat{T}^{\mu\nu}(x)] \\ &= \sum_{\lambda, \lambda'} \int d^2\mathbf{R}_\perp \mathcal{Q}^{\mu\nu}_{\alpha\beta}(\mathbf{R}_\perp, \tau; \lambda, \lambda') \\ &\quad \times t^{\alpha\beta}(\mathbf{x}_\perp - \mathbf{R}_\perp; \lambda, \lambda'), \end{aligned} \quad (20)$$

where here $t^{\alpha\beta}$ is the intrinsic EMT and $\mathcal{Q}^{\mu\nu}_{\alpha\beta}$ is the smearing function.

In Ref. [33], we gave explicit formulas for individual components of the intrinsic current and associated smearing functions. The formulas given therein can be written more compactly as

$$\begin{aligned} \mathcal{P}^\mu_\nu(\mathbf{R}_\perp, \tau; \lambda, \lambda') &= \int \frac{d^3\mathbf{P}}{2P_z(2\pi)^3} \int \frac{d^2\Delta_\perp}{(2\pi)^2} \langle \mathbf{p}, \lambda | \hat{\rho} | \mathbf{p}', \lambda' \rangle \\ &\quad \times \frac{m}{P_z} \bar{\Lambda}^\mu_\nu e^{i\Delta_0\tau} e^{-i\Delta_\perp \cdot \mathbf{R}_\perp} \Big|_{\Delta_z=0} \end{aligned} \quad (21)$$

for the smearing function, where $\Delta_0 = p'_0 - p_0 = (\mathbf{P} \cdot \Delta_\perp) / P_z$ and

$$\begin{aligned} j^\mu(\mathbf{b}_\perp; \lambda, \lambda') &= \int \frac{d^2\Delta_\perp}{(2\pi)^2} (\bar{\Lambda}^{-1})^\mu_\nu \frac{\langle \mathbf{p}', \lambda' | \hat{J}^\nu(0) | \mathbf{p}, \lambda \rangle}{2m} \\ &\quad \times e^{-i\Delta_\perp \cdot \mathbf{b}_\perp} \Big|_{\Delta_z=0} \end{aligned} \quad (22)$$

¹Reference [33] used three-dimensional smearing functions depending on \mathbf{R} , but since the R^3 coordinate does not appear in the intrinsic density, no information is lost by using $\mathcal{P}^\mu_\nu(\mathbf{R}_\perp, \tau) \equiv \int dR^3 (\mathcal{P}_{3D})^\mu_\nu(\mathbf{R}, \tau)$ instead.

for the intrinsic electromagnetic current. Here, $\mathbf{b}_\perp = \mathbf{x}_\perp - \mathbf{R}_\perp$ is the impact parameter, and additional momentum variables are given by $P = \frac{1}{2}(p + p')$ and $\Delta = p' - p$. The matrix $\bar{\Lambda}$ appearing in these formulas is given by

$$\bar{\Lambda}^\mu{}_\nu = \begin{bmatrix} P_z/m & 0 & 0 & 0 \\ P_x/m & 1 & 0 & 0 \\ P_y/m & 0 & 1 & 0 \\ (P_z - P_0)/m & -P_x/P_z & -P_y/P_z & m/P_z \end{bmatrix}. \quad (23)$$

It should be noted that despite its similar appearance to Eq. (A15), $\bar{\Lambda}^\mu{}_\nu$ is not a Lorentz boost, as demonstrated by Eq. (B22).

For the energy-momentum tensor, the analogs of the equations above are

$$\begin{aligned} \mathcal{Q}^{\mu\nu}{}_{\alpha\beta}(\mathbf{R}_\perp, \tau; \lambda, \lambda') &= \int \frac{d^3\mathbf{P}}{2P_z(2\pi)^3} \int \frac{d^2\Delta_\perp}{(2\pi)^2} \langle \mathbf{p}, \lambda | \hat{\rho} | \mathbf{p}', \lambda' \rangle \\ &\times \frac{m}{P_z} \left(\bar{\Lambda}^\mu{}_\alpha \bar{\Lambda}^\nu{}_\beta - \frac{\Delta_\perp^2}{4P_z^2} \delta_3^\mu \delta_3^\nu \delta_\alpha^3 \delta_\beta^3 \right) \\ &\times e^{i\Delta_0\tau} e^{-i\Delta_\perp \cdot \mathbf{R}_\perp} \Big|_{\Delta_z=0} \end{aligned} \quad (24)$$

for the smearing function and

$$t^{\mu\nu}(\mathbf{b}_\perp; \lambda, \lambda') = \int \frac{d^2\Delta_\perp}{(2\pi)^2} \mathcal{R}^{\mu\nu}{}_{\alpha\beta} \frac{\langle \mathbf{p}', \lambda' | \hat{T}^{\alpha\beta}(0) | \mathbf{p}, \lambda \rangle}{2m} \times e^{-i\Delta_\perp \cdot \mathbf{b}_\perp} \Big|_{\Delta_z=0}, \quad (25a)$$

$$\begin{aligned} \mathcal{R}^{\mu\nu}{}_{\alpha\beta} &= (\bar{\Lambda}^{-1})^\mu{}_\alpha (\bar{\Lambda}^{-1})^\nu{}_\beta \\ &\times \begin{cases} 1 & : \mu \neq 3 \text{ or } \nu \neq 3 \\ \left(1 - \frac{\Delta_\perp^2}{4m^2}\right)^{-1} & : \mu = \nu = 3 \end{cases} \end{aligned} \quad (25b)$$

for the intrinsic EMT.

Equation (25) is the primary formula we shall employ throughout this work to obtain intrinsic EMT densities. A proof of this formula, along with proofs of Eqs. (21), (22), and (24), can be found in Appendix B.

IV. ENERGY-MOMENTUM TENSOR OF SPIN-ZERO TARGETS

Although we are primarily interested in the proton in this work, we consider the spin-zero target first as a warm-up exercise, since the resulting densities are simpler.

The standard form factor breakdown for the EMT of a spin-zero target is [15]

$$\begin{aligned} \langle \mathbf{p}' | \hat{T}^{\mu\nu}(0) | \mathbf{p} \rangle &= 2P^\mu P^\nu A(\Delta^2) \\ &+ \frac{1}{2} (\Delta^\mu \Delta^\nu - \Delta^2 g^{\mu\nu}) D(\Delta^2). \end{aligned} \quad (26)$$

From Eq. (25), it follows that the intrinsic EMT of a spin-zero target is

$$t^{\mu\nu}(\mathbf{b}_\perp) = m \int \frac{d^2\Delta_\perp}{(2\pi)^2} \left\{ \bar{n}^\mu \bar{n}^\nu A(-\Delta_\perp^2) + \left(\frac{\Delta_\perp^\mu \Delta_\perp^\nu + \Delta_\perp^2 g^{\mu\nu}}{4m^2} \right) D(-\Delta_\perp^2) \right\}, \quad (27)$$

where $\bar{n}^\mu = (1; 0, 0, 0)$ is defined to project out the zeroth component of a four-vector when written in covariant form (with a lower Lorentz index), e.g., $\bar{n}^\mu p_\mu = p_0$. The interpretations of individual components of the EMT were described in Sec. II; we shall presently analyze results for the components in terms of those interpretations.

A. Energy density

Consulting the dictionary of Eq. (17), the rest frame energy density for a spin-zero target is

$$\begin{aligned} \mathcal{E}(\mathbf{b}_\perp) &= t^{00}(\mathbf{b}_\perp) - t^{03}(\mathbf{b}_\perp) \\ &= m \int \frac{d^2\Delta_\perp}{(2\pi)^2} \left\{ A(-\Delta_\perp^2) + \frac{\Delta_\perp^2}{4m^2} D(-\Delta_\perp^2) \right\} e^{-i\Delta_\perp \cdot \mathbf{b}_\perp}. \end{aligned} \quad (28)$$

This is a new result. Although *a priori* results exist for energy densities of spin-zero [31] and spin-half [16] targets in standard light front coordinates, the tilted coordinate energy is different from the light front energy, so naturally Eq. (28) differs from the light front energy density in Ref. [31]. In fact, the energy in tilted light front coordinates is equal to the more familiar instant form energy [33], for which Eq. (28) provides a two-dimensional relativistic density in the target's rest frame.

Integrating Eq. (28) gives m as the total energy, as expected for a system at rest. Additionally, Eq. (28) can be used to define a rest frame energy radius:

$$\begin{aligned} \langle \mathbf{b}_\perp^2 \rangle_{\text{energy}} &\equiv \frac{1}{m} \int d^2\mathbf{b}_\perp \mathbf{b}_\perp^2 \mathcal{E}(\mathbf{b}_\perp) \\ &= 4 \frac{dA(\Delta^2)}{d\Delta^2} \Big|_{\Delta^2=0} - \frac{1}{m^2} D(0). \end{aligned} \quad (29)$$

B. Momentum density

From the dictionary in Eq. (17), the momentum density is given by

$$\begin{aligned} \mathcal{P}(\mathbf{b}_\perp) &= t^{01}(\mathbf{b}_\perp) \hat{e}_x + t^{02}(\mathbf{b}_\perp) \hat{e}_y + t^{00}(\mathbf{b}_\perp) \hat{e}_z \\ &= m \hat{e}_z \int \frac{d^2\Delta_\perp}{(2\pi)^2} A(-\Delta_\perp^2) e^{-i\Delta_\perp \cdot \mathbf{b}_\perp}, \end{aligned} \quad (30)$$

which is nonzero only for the longitudinal momentum. Significantly, the z momentum in tilted coordinates is equal to the plus momentum in light front coordinates: $P_z = P_{\text{LF}}^+$. It is thus not surprising that the momentum density we find is equal to prior results for the light front momentum density [17] upon setting $P_{\text{LF}}^+ \rightarrow m$.

It is worth stressing (see Ref. [33] and Appendix A) that—in tilted coordinates— P_z is equal to m rather than 0 at rest. Thus, a nonzero P_z density does not indicate motion within the system. Rather than a density for a quantity of motion, the P_z density can be interpreted as an inertia density, since classically, contravariant components of the tilted momentum and the velocity are related by $p^i = p_z v^i$. On the other hand, the energy fluxes t^i_0 have a clearer interpretation as encoding motion within the system. We shall look at these next.

C. Energy flux density

From the dictionary in Eq. (17), the energy flux density is given by

$$\mathcal{F}_E(\mathbf{b}_\perp) = (t^{i0}(\mathbf{b}_\perp) - t^{i3}(\mathbf{b}_\perp))\hat{e}_i = 0, \quad (31)$$

which is identically zero.

D. Stress tensor

Using the dictionary in Eq. (17), the stress tensor for a spin-zero target is

$$\begin{aligned} S^{ij}(\mathbf{b}_\perp) &= t^{i1}\delta^{j1} + t^{i2}\delta^{j2} + t^{i0}\delta^{j3} \\ &= \frac{1}{4m} \int \frac{d^2\Delta_\perp}{(2\pi)^2} (\Delta_\perp^i \Delta_\perp^j - \delta^{ij} \Delta_\perp^2) D(-\Delta_\perp^2) e^{-i\Delta_\perp \cdot \mathbf{b}_\perp}. \end{aligned} \quad (32)$$

The transverse components $i, j \in \{1, 2\}$ of the stress tensor by themselves reproduce prior results for the transverse light front stress tensor [17] if one sets $P_{\text{LF}}^+ \rightarrow m$.

More remarkably, however, there is apparently a new longitudinal pressure,

$$p_z(\mathbf{b}_\perp) \equiv S^{33}(\mathbf{b}_\perp) = - \int \frac{d^2\Delta_\perp \Delta_\perp^2}{(2\pi)^2 4m} D(-\Delta_\perp^2) e^{-i\Delta_\perp \cdot \mathbf{b}_\perp}, \quad (33)$$

where, as is standard in continuum mechanics [51–53, 55–57], normal stresses are called pressures. Shear stresses involving the z direction, which would correspond to fluxes of P_z in the transverse plane or longitudinal fluxes of \mathbf{P}_\perp , vanish for the spin-zero target. This is likely a consequence of the z coordinate dependence being integrated out, as integrating out x or y likewise leads to the elimination of shear stresses in integrated-out direction.

V. ENERGY-MOMENTUM TENSOR OF SPIN-HALF TARGETS

Since our primary objective is to obtain energy-momentum densities and currents for the proton, we proceed to consider spin-half targets. We primarily focus on the symmetric Belinfante EMT, but will briefly consider how the formalism changes when the asymmetric EMT is instead used in Sec. V F.

The standard form factor breakdown for the symmetric EMT for spin-half targets is [15]

$$\begin{aligned} \langle \mathbf{p}', \lambda' | \hat{T}^{\mu\nu}(0) | \mathbf{p}, \lambda \rangle &= \bar{u}(\mathbf{p}', \lambda') \left\{ \frac{\gamma^{\{\mu} P^{\nu\}}}{2} A(\Delta^2) + \frac{i P^{\{\mu} \sigma^{\nu\} \rho} \Delta_\rho}{4m} B(\Delta^2) \right. \\ &\quad \left. + \frac{\Delta^\mu \Delta^\nu - g^{\mu\nu} \Delta^2}{4m} D(\Delta^2) \right\} u(\mathbf{p}, \lambda). \end{aligned} \quad (34)$$

Using formulas from Appendix A of Ref. [33], we can explicitly evaluate matrix elements of the EMT when $\Delta_z = 0$ to be

$$\begin{aligned} \langle \mathbf{p}', \lambda' | \hat{T}^{\mu\nu}(0) | \mathbf{p}, \lambda \rangle &= 2P^\mu P^\nu \left\{ (\sigma_0)_{\lambda'\lambda} A(-\Delta_\perp^2) - \frac{i \epsilon^{\alpha\beta\gamma\delta} n_\alpha \bar{n}_\beta \Delta_\gamma (\sigma_\delta)_{\lambda'\lambda}}{2m} B(-\Delta_\perp^2) \right\} \\ &\quad + \left\{ - \frac{i P^{\{\mu} \epsilon^{\nu\} \rho\sigma\tau} n_\rho P_\sigma \Delta_\tau}{(P \cdot n)} (\sigma_3)_{\lambda'\lambda} + \frac{m P^{\{\mu} n^{\nu\}}}{(P \cdot n)} i \epsilon^{\alpha\beta\gamma\delta} n_\alpha \bar{n}_\beta \Delta_\gamma (\sigma_\delta)_{\lambda'\lambda} \right\} J(-\Delta_\perp^2) \\ &\quad + \frac{\Delta^\mu \Delta^\nu - g^{\mu\nu} \Delta^2}{2} \left((\sigma_0)_{\lambda'\lambda} + \frac{i \epsilon^{\alpha\beta\gamma\delta} n_\alpha \bar{n}_\beta \Delta_\gamma (\sigma_\delta)_{\lambda'\lambda}}{2m} \right) D(-\Delta_\perp^2), \end{aligned} \quad (35)$$

where

$$J(\Delta^2) = \frac{1}{2} (A(\Delta^2) + B(\Delta^2)) \quad (36)$$

is the angular momentum form factor [15]. Using Eq. (25) for the intrinsic EMT of a general system then gives

$$\begin{aligned}
t^{\mu\nu}(\mathbf{b}_\perp; \lambda, \lambda') = m \int \frac{d^2\Delta_\perp}{(2\pi)^2} & \left\{ \bar{n}^\mu \bar{n}^\nu \left((\sigma_0)_{\lambda\lambda'} A(-\Delta_\perp^2) + \frac{(\boldsymbol{\sigma}_{\lambda\lambda'} \times \mathbf{i}\Delta_\perp) \cdot \hat{e}_z}{2m} B(-\Delta_\perp^2) \right) \right. \\
& \left. + \frac{\bar{n}^{\{\mu} (\boldsymbol{\sigma}_{\lambda\lambda'} \times \mathbf{i}\Delta_\perp)^{\nu\}}}{2m} J(-\Delta_\perp^2) + \left(\frac{\Delta_\perp^\mu \Delta_\perp^\nu + g^{\mu\nu} \Delta_\perp^2}{4m^2} \right) \left((\sigma_0)_{\lambda\lambda'} - \frac{(\boldsymbol{\sigma}_{\lambda\lambda'} \times \mathbf{i}\Delta_\perp) \cdot \hat{e}_z}{2m} \right) D(-\Delta_\perp^2) \right\}. \quad (37)
\end{aligned}$$

As with the spin-zero target, we will use the dictionary in Eq. (17) to obtain energy and momentum densities and currents from the intrinsic EMT. We will find the nine Galilean components of the EMT—that is, the momentum densities and transverse stress tensor—reproduce results from standard light front coordinates, but the energy density, P_z fluxes, and longitudinal energy flux are newly found.

A. Momentum densities

We consider the momentum densities first. It is instructive to consider the P_z density and \mathbf{P}_\perp densities in separate equations, as their behavior is quite different. From Eqs. (25) and (37), we find these densities to be

$$\begin{aligned}
\mathcal{P}_z(\mathbf{b}_\perp, \hat{\mathbf{s}}) &= -t^0_3 \\
&= m \int \frac{d^2\Delta_\perp}{(2\pi)^2} \left(A(-\Delta_\perp^2) + \frac{(\hat{\mathbf{s}} \times \mathbf{i}\Delta_\perp) \cdot \hat{e}_z}{2m} B(-\Delta_\perp^2) \right) \\
&\quad \times e^{-\mathbf{i}\Delta_\perp \cdot \mathbf{b}_\perp}, \quad (38a)
\end{aligned}$$

$$\begin{aligned}
\mathcal{P}_\perp(\mathbf{b}_\perp, \hat{\mathbf{s}}) &= -t^0_1 \hat{e}_x - t^0_2 \hat{e}_y \\
&= m(\hat{\mathbf{s}} \cdot \hat{e}_z) \int \frac{d^2\Delta_\perp}{(2\pi)^2} \frac{\hat{e}_z \times \mathbf{i}\Delta_\perp}{2m} J(-\Delta_\perp^2) e^{-\mathbf{i}\Delta_\perp \cdot \mathbf{b}_\perp}. \quad (38b)
\end{aligned}$$

The P_z density reproduces prior results for the P^+ density in standard light front coordinates [63] if one sets $P^+ \rightarrow m$. For a free point fermion, $A(\Delta^2) = 1$ and $B(\Delta^2) = 0$, so the P_z density just becomes $m\delta^{(2)}(\mathbf{b}_\perp)$. This is expected because P_z is the central charge of the Galilean subgroup and is preserved by transverse boosts, so the barycentric coordinate \mathbf{R}_\perp is a center-of- P_z coordinate and the intrinsic densities are relative to the center of P_z . (This has been explained in terms of standard light front coordinates by Lorcé [64].)

For nonpointlike targets with $B(\Delta^2) \neq 0$, transversely polarized states will exhibit azimuthal modulations in the P_z density. The behavior is analogous to the modulations in its charge density [33] and is likewise induced by the synchronization scheme—specifically by modulations in the apparent clock rate of matter revolving around the target's center. It is worth pointing out that $F_2(\Delta^2)$ —which controls the charge density modulations—and $B(\Delta^2)$ are Mellin moments of the same generalized parton distribution

(GPD) $E(x, \xi, \Delta^2)$, suggesting that this GPD has an interpretation in terms of encoding partonic motion.

Despite the presence of these modulations, there is not a P_z dipole moment. This would, of course, contradict the barycenter being the center of P_z . If one calculates the P_z dipole moment from Eq. (38),

$$\langle \mathbf{b}_\perp \rangle_{P_z} = \int d^2\mathbf{b}_\perp \mathbf{b}_\perp \mathcal{P}_z(\mathbf{b}_\perp, \hat{\mathbf{s}}) = \frac{\hat{e}_z \times \hat{\mathbf{s}}}{2} B(0). \quad (39)$$

However, $B(0) = 0$, a fact known as the vanishing of the anomalous gravitomagnetic moment [65]. It follows from the simultaneous sum rules $A(0) = 1$ (the momentum sum rule) and $J(0) = \frac{1}{2}$ (the angular momentum sum rule).

A radius can be associated with the P_z density

$$\langle \mathbf{b}_\perp^2 \rangle_{P_z} = \frac{1}{m} \int d^2\mathbf{b}_\perp \mathbf{b}_\perp^2 \mathcal{P}_z(\mathbf{b}_\perp, \hat{\mathbf{s}}) = 4 \left. \frac{dA(\Delta^2)}{d\Delta^2} \right|_{\Delta^2=0}. \quad (40)$$

This radius has appeared in the literature before. It has been called a P^+ radius in standard light front coordinates [17], and occasionally called a mass radius. [As pointed out by Lorcé *et al.* [8], mass plays several roles in relativity, and the P^+ radius could be considered a kind of mass radius. This is distinct, however, from the energy radius, which we give in Eq. (46).]

The \mathbf{P}_\perp density in Eq. (38) would be the same in standard light front coordinates being a Galilean component of the EMT, but to the best of our knowledge this result has not been previously reported. This density is related to and tracks the z component of the *total* angular momentum density, the latter being

$$\mathcal{J}_z(\mathbf{b}_\perp, \hat{\mathbf{s}}) = (\mathbf{b}_\perp \times \mathcal{P}_\perp(\mathbf{b}_\perp, \hat{\mathbf{s}})) \cdot \hat{e}_z. \quad (41)$$

This may appear counterintuitive on first sight, as it superficially resembles the formula $\mathbf{r} \times \mathbf{p}$ for the *orbital* angular momentum of a body. However, the symmetric Belinfante EMT appears as the source of gravitation in general relativity, and the equivalence principle implies that all angular momentum should gravitate the same way. Thus, neither the Belinfante EMT nor its associated densities should be able to distinguish between spin and orbital angular momentum (OAM).

Moreover, despite the superficial resemblance, the right-hand side of Eq. (41) does not give an OAM density—at least not in terms of how OAM is usually defined. The amount of momentum $\mathcal{P}_\perp(\mathbf{b}_\perp, \hat{\mathbf{s}}) d^2\mathbf{b}_\perp$ contained in a small

spatial region $d^2\mathbf{b}_\perp$ is not necessarily the momentum carried by a constituent of the target. This is especially clear if the target under consideration is a pointlike particle. The particle itself is an excitation of a field, which is the more fundamental object in quantum field theory. The momentum element $\mathcal{P}_\perp(\mathbf{b}_\perp, \hat{s})d^2\mathbf{b}_\perp$ is the amount of momentum carried by the field in this small spatial region. However, the only particle present is the target itself, which is at rest, so the OAM is zero. Thus Eq. (41) does not encode an OAM density.

B. Energy fluxes

From Eqs. (25) and (37), we find the energy fluxes to be

$$\begin{aligned}\mathcal{F}_E(\mathbf{b}_\perp, \hat{s}) &= t^i_0 \hat{e}_i \\ &= m \int \frac{d^2\Delta_\perp}{(2\pi)^2} \frac{\hat{s} \times i\Delta_\perp}{2m} J(-\Delta_\perp^2) e^{-i\Delta_\perp \cdot \mathbf{b}_\perp}.\end{aligned}\quad (42)$$

There is an energy flux due to the presence of angular momentum in the system, which is intuitively sensible. The transverse energy flux in particular is equal to the transverse momentum density. This mimics the well-known fact that the symmetric EMT in instant form coordinates has identical momentum densities and energy fluxes.

C. Stress tensor and momentum fluxes

We next consider the intrinsic stress tensor of a spin-half target. From Eqs. (25) and (37),

$$\begin{aligned}S^{ij}(\mathbf{b}_\perp, \hat{s}) &\equiv -t^i_j(\mathbf{b}_\perp) \\ &= m\delta^{3j} \int \frac{d^2\Delta_\perp}{(2\pi)^2} \frac{(\hat{s} \times i\Delta_\perp)^i}{2m} J(-\Delta_\perp^2) e^{-i\Delta_\perp \cdot \mathbf{b}_\perp} \\ &\quad + \frac{1}{4m} \int \frac{d^2\Delta_\perp}{(2\pi)^2} (\Delta_\perp^i \Delta_\perp^j - \delta^{ij} \Delta_\perp^2) \\ &\quad \times \left[1 - \frac{(\hat{s} \times i\Delta_\perp) \cdot \hat{e}_z}{2m} \right] D(-\Delta_\perp^2) e^{-i\Delta_\perp \cdot \mathbf{b}_\perp}.\end{aligned}\quad (43)$$

We have broken the result into two pieces, the first of which depends on the angular momentum form factor $J(\Delta^2)$, and the other of which depends on the form factor $D(\Delta^2)$.

The first angular momentum piece of the stress tensor introduces asymmetric shear stresses. Recalling that the stress tensor consists of momentum fluxes, this piece of the stress tensor encodes fluxes of P_z in all three spatial directions, but not of \mathbf{P}_\perp . Now, a major difference between P_z and \mathbf{P}_\perp in tilted coordinates is that the former is nonzero even if the velocity is zero; a P_z flux cannot be interpreted as a flux of some quantity of motion. Since classically $\mathbf{p}_\perp = p_z \mathbf{v}_\perp$ and $p_z - E = p_z v_z$ (these relations can be found in Appendix A), it should perhaps be the P_z flux minus the energy flux that is compared to the \mathbf{P}_\perp flux:

$$\begin{aligned}\mathcal{F}_{p_z}(\mathbf{b}_\perp, \hat{s}) - \mathcal{F}_E(\mathbf{b}_\perp, \hat{s}) \\ = -m\hat{e}_z \int \frac{d^2\Delta_\perp}{(2\pi)^2} \frac{\Delta_\perp^2}{4m} \left[1 - \frac{(\hat{s} \times i\Delta_\perp) \cdot \hat{e}_z}{2m} \right] D(-\Delta_\perp^2) e^{-i\Delta_\perp \cdot \mathbf{b}_\perp}.\end{aligned}\quad (44)$$

For comparison, the transverse components of the stress tensor are

$$\begin{aligned}S^i_j(\mathbf{b}_\perp, \hat{s}) &= \frac{1}{4m} \int \frac{d^2\Delta_\perp}{(2\pi)^2} (\Delta_\perp^i \Delta_\perp^j - \delta^{ij} \Delta_\perp^2) \\ &\quad \times D(-\Delta_\perp^2) e^{-i\Delta_\perp \cdot \mathbf{b}_\perp}.\end{aligned}\quad (45)$$

Both of these include only the form factor $D(\Delta^2)$, which vanishes in the case of a pointlike particle [66] and can be interpreted as encoding internal dynamics in composite fermions [66]. For pointlike fermions, then, the energy and P_z fluxes are not zero, but are instead equal, and differences between them are an indication of dynamics and internal motion.

As a last remark, we note that the transverse P_z flux is equal to the \mathbf{P}_\perp density, i.e., $\mathcal{F}_{p_z}^{(\perp)}(\mathbf{b}_\perp, \hat{s}) = \mathcal{P}_\perp(\mathbf{b}_\perp, \hat{s})$. This seems to comport with the classical tilted coordinate relation $\mathbf{p}_\perp = p_z \mathbf{v}_\perp$ if it is applied to the momentum carried by the target in any small region of space. Since this was a classical relation derived for observable bodies that obey the mass-shell relation $p^2 = m^2$, it is not a formal necessity that small elements of momenta supported by an infinitesimal region of space obey this relation, but it is interesting to note.

D. Energy density

The last component of the intrinsic EMT to consider is the energy density. From Eqs. (25) and (37), using $\mathcal{E}(\mathbf{b}_\perp, \hat{s}) = t^0_0(\mathbf{b}_\perp, \hat{s})$ gives exactly Eq. (2) given in the Introduction. The spin-independent piece of the spin-half energy density is identical to the spin-zero energy density of Eq. (28). The spin-dependent piece does not contribute to the energy radius, which is therefore identical to the spin-zero case:

$$\begin{aligned}\langle \mathbf{b}_\perp^2 \rangle_{\text{energy}} &\equiv \frac{1}{m} \int d^2\mathbf{b}_\perp \mathbf{b}_\perp^2 \mathcal{E}(\mathbf{b}_\perp, \hat{s}) \\ &= 4 \frac{dA(\Delta^2)}{d\Delta^2} \Big|_{\Delta^2=0} - \frac{1}{m^2} D(0).\end{aligned}\quad (46)$$

The spin-dependent part of the EMT introduces angular modulations through several of the form factors, which must be attributed to distinct physical effects. The angular modulations introduced through the form factor $B(\Delta^2)$ can be attributed to clock rate modulations, as explained for the P_z density in Sec. V A. In particular, modulations due to $B(\Delta^2)$ will increase density on the side of the hadron moving away from the observer.

The angular momentum form factor $J(\Delta^2)$ contributes to angular modulations with the opposite sign from $B(\Delta^2)$, thus causing the density to increase on the side moving toward the observer. This is effectively an artifact of the density being defined with respect to the center of P_z . Since $B(0) = 0$, the amount of P_z on each side of the spin axis in a transversely polarized fermion is the same. If the classical relation $p_z - E = p_z v_z$ is assumed to hold for each half of the fermion, the half moving toward the observer has $v_z < 0$ and thus should have greater energy, and the half moving away should have less energy. The modulations in the energy density arising from $J(\Delta^2)$ accomplish just this. In fact, by comparing Eqs. (43), (43), and (2) we find

$$\mathcal{P}_z(\mathbf{b}_\perp, \hat{s}) - \mathcal{E}(\mathbf{b}_\perp, \hat{s}) = \hat{e}_z \cdot \mathcal{F}_{p_z}(\mathbf{b}_\perp, \hat{s}), \quad (47)$$

meaning that $p_z - E = p_z v_z$ apparently holds for infinitesimal elements of the hadron everywhere on the transverse plane.

In contrast to the P_z density, the energy density entails a synchronization-induced energy dipole moment:

$$\begin{aligned} \mathbf{d}_E &\equiv \langle \mathbf{b}_\perp \rangle_E = \int d^2 \mathbf{b}_\perp \mathbf{b}_\perp \mathcal{E}(\mathbf{b}_\perp, \hat{s}) \\ &= -\frac{\hat{e}_z \times \hat{s}}{2} J(0) = -\frac{1}{4} \hat{e}_z \times \hat{s}. \end{aligned} \quad (48)$$

We reiterate and stress that this apparent dipole moment arises from the proton's ‘‘center’’ being given by the center of P_z rather than the center of energy. However, the remaining modulations from the form factors $B(t)$ and $D(t)$ —which do not contribute to the dipole moment—may be due to clock rate modulations, similar to the modulations in the P_z density.

E. Numerical estimates for the proton

We now consider what the energy and momentum densities and currents might look like for the proton. Currently, high-precision empirical results for the proton's gravitational form factors do not exist. We shall thus utilize reasonable model estimates instead.

It is known from holographic QCD models [67–69] that the pole structures of the gravitational form factors are dominated by an infinite tower of $J^{PC} = 0^{++}$ and 2^{++} glueball resonances—referred to as ‘‘glueball dominance’’ by Fujita *et al.* [69], in analogy to the well-known vector meson dominance [70,71] of electromagnetic form factors. Fujita *et al.* also note that simple multipole forms can reasonably approximate such an infinite tower, as has been shown explicitly for holographic models of electromagnetic form factors [72]. Mamo and Zahed [68] in particular find that the gravitational form factors in their holographic

model can be reasonably estimated by the simple functional forms²

$$A(-\Delta_\perp^2) \approx \frac{1}{(1 + \Delta_\perp^2/\tilde{m}_T^2)^2}, \quad (49a)$$

$$B(-\Delta_\perp^2) \approx 0, \quad (49b)$$

$$D(-\Delta_\perp^2) \approx D(0) \frac{1 + \frac{\Delta_\perp^2}{4\tilde{m}_T^2} + \frac{\Delta_\perp^2}{4\tilde{m}_S^2}}{(1 + \Delta_\perp^2/\tilde{m}_T^2)^2 (1 + \Delta_\perp^2/\tilde{m}_S^2)^2}, \quad (49c)$$

where $D(0) = -4$, $\tilde{m}_T = 1.124$ GeV, and $\tilde{m}_S = 1$ GeV. We remark that these form factors are compatible with lattice data [73] and with recent empirical measurements of J/ψ photoproduction the $J/\psi - 007$ experiment [74]. Additionally, the large- t falloff of these form factors follows the expected behavior from perturbative QCD [75].

Because $B(t) = 0$ in the example we consider, the P_z density is independent of polarization and is equal to

$$\mathcal{P}_z(\mathbf{b}_\perp, \hat{s}) = \frac{\tilde{m}_T^3 m b_\perp}{4\pi} K_1(\tilde{m}_T b_\perp), \quad (50)$$

where $K_\nu(x)$ is a modified Bessel function of the second kind [76]. It is worth noting that this density is finite at the origin:

$$\lim_{b_\perp \rightarrow 0} \mathcal{P}_z(\mathbf{b}_\perp, \hat{s}) = \frac{\tilde{m}_T^2 m}{4\pi}, \quad (51)$$

in contrast to the 2D Fourier transform of a monopole form [77].

The transverse momentum density is given by

$$\mathcal{P}_\perp(\mathbf{b}_\perp, \hat{s}) = \frac{(\hat{s} \cdot \hat{e}_z)(\hat{e}_y \cos \phi - \hat{e}_x \sin \phi)}{16\pi} \tilde{m}_T^4 b_\perp K_0(\tilde{m}_T b_\perp), \quad (52)$$

from which it follows that the density of the z component of angular momentum is

$$\mathcal{J}_z(\mathbf{b}_\perp, \hat{s}) = \frac{(\hat{s} \cdot \hat{e}_z) b_\perp^2 \tilde{m}_T^4}{16\pi} K_0(\tilde{m}_T b_\perp). \quad (53)$$

Numerical results for the momentum and angular momentum densities for a longitudinally polarized proton are presented in Fig. 2. The P_z density is unchanged for

²We note that Mamo and Zahed [68] use $A(0) = 0.53$ in their work rather than $A(0) = 1$ as we use here because they are describing only the gluonic contributions to the gravitational form factors. The estimates we present are for the total energy-momentum tensor, including both quark and gluon contributions, so we simply use their functional form for the Δ_\perp dependence while imposing the momentum sum rule $A(0) = 1$.

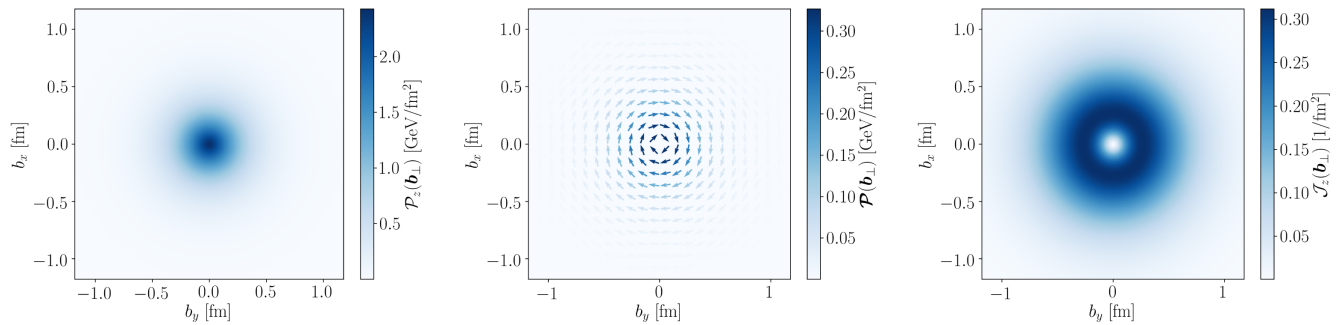


FIG. 2. Momentum and angular momentum densities in a proton. (Left panel) The P_z density, which is independent of polarization under the assumption $B(t) = 0$. (Middle panel) The \mathbf{P}_\perp density in a proton that is spin-up along the z axis. (Right panel) The J_z (angular momentum) density in a proton that is spin-up along the z axis. In these plots, the x axis is oriented vertically and the y axis horizontally so that the z axis points into the page, allowing plots to mimic what an observer would see at fixed light front time.

transversely polarized protons owing to the assumption $B(t) = 0$, while the \mathbf{P}_\perp and J_z densities vanish identically for transversely polarized protons. The angular momentum density has an apparent hole in it because $b_\perp^2 K_0(\tilde{m}_T b_\perp)$ vanishes at the origin.

The energy and momentum flux densities are our next consideration. The transverse components of the stress tensor have previously been considered in Refs. [16,17,47,78], with Ref. [47] in particular exploring the distortions in eigenpressure directions that occur in transversely polarized states. Since tilted coordinates newly allow access to energy and P_z flux densities, we will focus on these specifically.

As explained in Sec. V C, the transverse P_z flux is equal to the \mathbf{P}_\perp density; and as pointed out in Sec. V B, it is also equal to the transverse energy flux due to symmetry of the EMT. We thus point the reader to the middle panel of Fig. 2 for an estimate of these quantities for a longitudinally polarized proton.

The longitudinal P_z flux, which can also be interpreted as pressure in the z direction (since it is a normal stress) can be obtained by putting Eq. (49) into Eq. (43) with

$i = j = 3$. One can similarly obtain the longitudinal energy flux by plugging Eq. (49) into Eq. (42) with $i = 3$. Numerical results of taking these 2D Fourier transforms are presented in Fig. 3.

The longitudinal flux densities all integrate to zero, which may be difficult to see by eye in the P_z flux plots; the core of negative P_z flux is surrounded by a diffuse cloud of positive flux. A one-dimensional reduction of P_z flux density for longitudinally polarized protons is presented later in Fig. 5, where the vanishing of the net flux is easier to see.

Finally, from Eqs. (2) and (49) we obtain the energy density. Numerical results for the energy density of both longitudinally and transversely polarized states are presented in Fig. 4. The right panel in particular shows the energy density of a transversely polarized proton with its spin-up along the x axis. In these plots, the x axis is vertical and the y axis horizontal, so that the z axis points into the page by the right-hand rule. This is done so that the plots are representative of what an observer would actually see at fixed light front time. The energy is lopsided on the side of

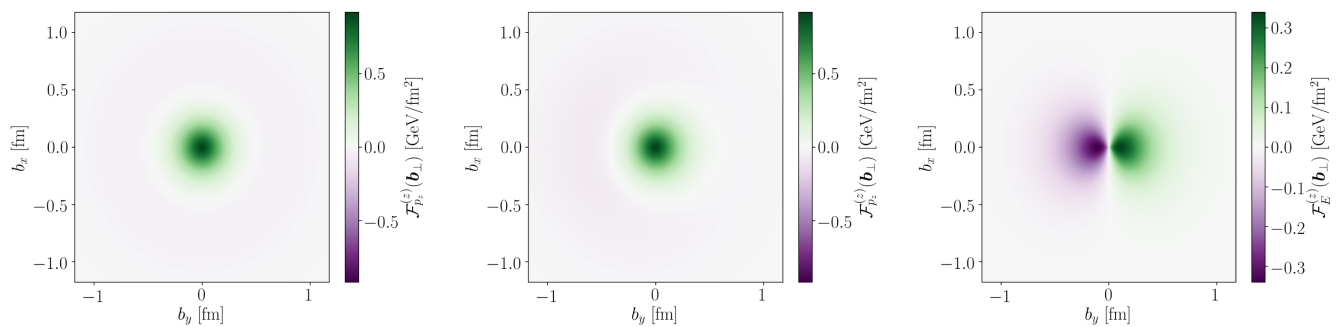


FIG. 3. P_z and energy flux densities in the z direction. The left panel shows the P_z flux density for a longitudinally polarized state, while the middle panel shows the same for a transversely polarized state with spin-up along the x axis. The right panel shows the longitudinal energy flux for this same transversely polarized state. The longitudinal energy flux is identically zero for a longitudinally polarized state (since energy flux is carried by angular momentum), and is thus not plotted. In these plots, the x axis is oriented vertically and the y axis horizontally so that the z axis points into the page, allowing plots to mimic what an observer would see at fixed light front time. Accordingly, positive flux is into the page (away from the observer) and negative flux is out of the page (toward the observer).

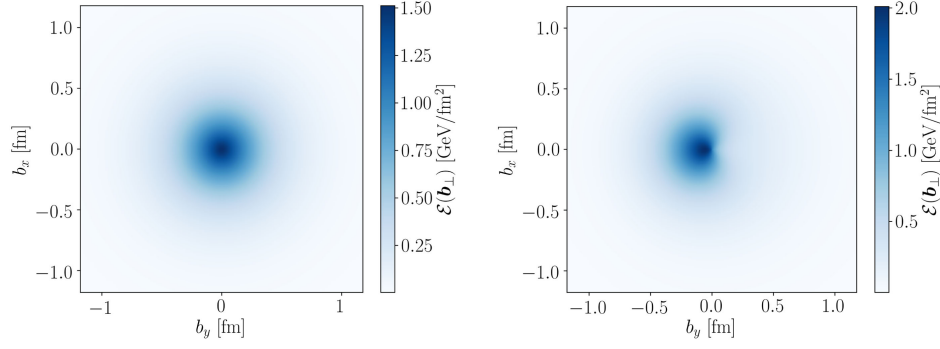


FIG. 4. Energy density for protons polarized with spin-up along the z axis (left panel) and spin-up along the x axis (right panel). In these plots, the x axis is oriented vertically and the y axis horizontally so that the z axis points into the page, allowing plots to mimic what an observer would see at fixed light front time.

the proton that is revolving toward the observer, in contrast to the modulations previously seen in the proton's charge density [33]. As explained in Sec. VD, these modulations have a different cause than the charge density modulations, which were the result of clock rate modulations. The energy density modulations are largely an artifact of the proton's center in the light front formalism being the center of P_z : there are equal amounts of P_z on both sides of the proton, and given the tilted coordinate relation $p_z v_z = p_z - E$, there must be more energy on the side with $v_z < 0$ —i.e., the side moving toward the observer.

It is also instructive to consider one-dimensional reductions of the densities and currents we have calculated. Such reductions are presented in Fig. 5, specifically for the case of a longitudinally polarized proton. This figure illustrates several interesting qualitative features of the energy and momentum densities. First of all, the magnitude of the transverse momentum density is much smaller than the P_z or energy densities. The P_z density, it should be recalled, is

not a measure of motion in tilted coordinates, but can better be interpreted as a measure of inertia, and, in fact, the P_z density here integrates to the mass. It is thus not surprising that the P_z density is much larger than the P_\perp density. On the contrary, the P_\perp density is quite large, becoming as large as hundreds of MeV/fm, which is indicative of ultrarelativistic motion within the proton.

Figure 5 also qualitatively illustrates that the energy distribution in the proton is broader than the P_z distribution. Accordingly, the energy radius should be larger than the momentum radius. Using Eqs. (40) and (46) for the radii, we find

$$\langle b_\perp^2 \rangle_{P_z} = (0.50 \text{ fm})^2, \quad (54a)$$

$$\langle b_\perp^2 \rangle_E = (0.65 \pm 0.02 \text{ fm})^2. \quad (54b)$$

We stress that these are just illustrative, and not the result of a precision calculation or extraction from precision empirical data. Future experiments aimed at extracting generalized parton distributions, such as deeply virtual Compton scattering [22–24,79] and single-diffractive hard exclusive reactions [80], must be carried out to provide both more realistic estimates of the proton's gravitational form factors.

Last, it is more apparent by eye in Fig. 5 that the longitudinal P_z flux integrates to zero than in the left panel of Fig. 3.

F. Changes when using the asymmetric EMT

Before concluding, let us consider how the densities we have present would be modified by including an antisymmetric piece in the EMT, as defined in Eq. (8). This would introduce an additional form factor

$$\langle \mathbf{p}', \lambda' | \hat{T}_A^{\mu\nu}(0) | \mathbf{p}, \lambda \rangle = \bar{u}(\mathbf{p}', \lambda') \gamma^{[\mu} P^{\nu]} u(\mathbf{p}, \lambda) S(\Delta^2), \quad (55)$$

which must be added to the breakdown in Eq. (34). Using formulas from Appendix A of Ref. [33], we can explicitly evaluate matrix elements of this when $\Delta_z = 0$ to be

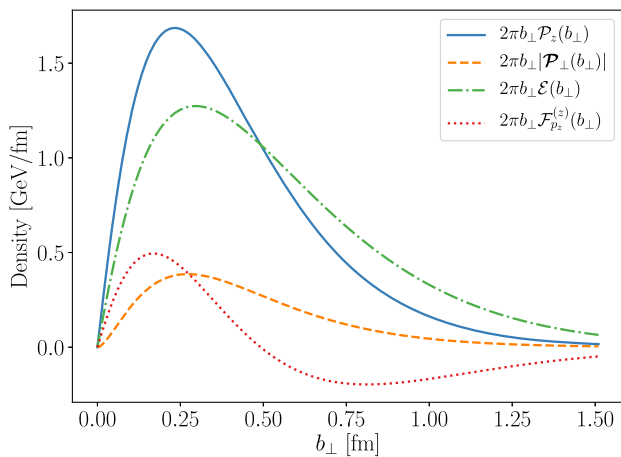


FIG. 5. One-dimensional reductions of several transverse densities in the proton. The solid blue line is the P_z density; the dashed orange line is the magnitude of the P_\perp density; the dash-dotted green line is the energy density; and the dotted red line is the longitudinal P_z flux.

$$\langle \mathbf{p}', \lambda' | \hat{T}_A^{\mu\nu}(0) | \mathbf{p}, \lambda \rangle = - \left\{ - \frac{i \mathbf{P}^{[\mu} \epsilon^{\nu] \rho \sigma \tau} n_\rho P_\sigma \Delta_\tau (\sigma_3)_{\lambda' \lambda}}{(P \cdot n)} + \frac{m \mathbf{P}^{[\mu} n^{\nu]}}{(P \cdot n)} i \epsilon^{\alpha \beta \gamma \delta} n_\alpha \bar{n}_\beta \Delta_\gamma (\sigma_\delta)_{\lambda' \lambda} \right\} S(-\Delta_\perp^2). \quad (56)$$

Using Eq. (25), the additional contribution of this anti-symmetric piece to the intrinsic EMT is

$$t^{\mu\nu}(\mathbf{b}_\perp; \lambda, \lambda') = -m \int \frac{d^2 \Delta_\perp}{(2\pi)^2} \frac{\bar{n}^{[\mu} (\boldsymbol{\sigma}_{\lambda' \lambda} \times \mathbf{i} \Delta_\perp)^{\nu]}}{2m} S(-\Delta_\perp^2). \quad (57)$$

Adding this to the intrinsic EMT would alter several of the densities we explored above. First, in the expression for the transverse momentum density $\mathcal{P}_\perp(\mathbf{b}_\perp, \hat{\mathbf{s}})$ in Eq. (38), the form factor $J(-\Delta_\perp^2)$ would be replaced by $J(-\Delta_\perp^2) - S(-\Delta_\perp^2)$, giving

$$\begin{aligned} \mathcal{P}_\perp^{(\text{asym})}(\mathbf{b}_\perp, \hat{\mathbf{b}}_\perp) &= \mathcal{P}_\perp(\mathbf{b}_\perp, \hat{\mathbf{b}}_\perp) \\ &\quad - m (\hat{e}_z \cdot \hat{\mathbf{s}}) \int \frac{d^2 \Delta_\perp}{(2\pi)^2} \frac{\hat{e}_z \times \mathbf{i} \Delta_\perp}{2m} \\ &\quad \times S(-\Delta_\perp^2) e^{-i \Delta_\perp \cdot \mathbf{b}_\perp}. \end{aligned} \quad (58)$$

Under the interpretation that $S(-\Delta_\perp^2)$ encodes the spatial distribution of *fermion* spin, the $J - S$ difference encodes a combination of quark OAM and gluon total angular momentum. Accordingly, when using the asymmetric EMT, the transverse momentum density tracks this particular mix of contributions to the angular momentum. If no gluons were present in the hadron, $J(-\Delta_\perp^2) - S(-\Delta_\perp^2)$ would simply track OAM. It is interesting to note that for a free fermion, this form factor difference is zero, and the transverse momentum density in a free fermion thus vanishes for the asymmetric EMT.

Second, in the energy flux density $\mathcal{F}_E(\mathbf{b}_\perp, \hat{\mathbf{s}})$ of Eq. (42), $J(-\Delta_\perp^2)$ would be replaced by $J(-\Delta_\perp^2) + S(-\Delta_\perp^2)$, giving

$$\begin{aligned} \mathcal{F}_E^{(\text{asym})}(\mathbf{b}_\perp, \hat{\mathbf{b}}_\perp) &= \mathcal{F}_E(\mathbf{b}_\perp, \hat{\mathbf{b}}_\perp) + m \int \frac{d^2 \Delta_\perp}{(2\pi)^2} \frac{\hat{\mathbf{s}} \times \mathbf{i} \Delta_\perp}{2m} \\ &\quad \times S(-\Delta_\perp^2) e^{-i \Delta_\perp \cdot \mathbf{b}_\perp}. \end{aligned} \quad (59)$$

Along the same vein, the P_z flux is also modified by replacing $J(-\Delta_\perp^2)$ with $J(-\Delta_\perp^2) + S(-\Delta_\perp^2)$ in Eq. (43) giving

$$\begin{aligned} \mathcal{F}_{p_z}^{(\text{asym})}(\mathbf{b}_\perp, \hat{\mathbf{b}}_\perp) &= \mathcal{F}_{p_z}(\mathbf{b}_\perp, \hat{\mathbf{b}}_\perp) \\ &\quad + m (\hat{e}_z \cdot \hat{\mathbf{s}}) \int \frac{d^2 \Delta_\perp}{(2\pi)^2} \frac{\hat{e}_z \times \mathbf{i} \Delta_\perp}{2m} \\ &\quad \times S(-\Delta_\perp^2) e^{-i \Delta_\perp \cdot \mathbf{b}_\perp}. \end{aligned} \quad (60)$$

Notably, the transverse P_z flux and transverse momentum densities are no longer equal for the asymmetric EMT, meaning small elements of matter inside the hadron no longer obey the relation $\mathbf{p}_\perp = p_z \mathbf{v}_\perp$. Of course, there is no formal constraint that formal elements of matter (as opposed to on-shell particles) must obey this relation, so the asymmetric EMT is not inconsistent for this.

Last, the energy density $\mathcal{E}(\mathbf{b}_\perp, \hat{\mathbf{s}})$ is modified in Eq. (2) by replacing $J(-\Delta_\perp^2)$ with $J(-\Delta_\perp^2) - S(-\Delta_\perp^2)$, giving

$$\begin{aligned} \mathcal{E}^{(\text{asym})}(\mathbf{b}_\perp, \hat{\mathbf{b}}_\perp) &= \mathcal{E}(\mathbf{b}_\perp, \hat{\mathbf{b}}_\perp) - m \int \frac{d^2 \Delta_\perp}{(2\pi)^2} \frac{\hat{e}_z \cdot (\hat{\mathbf{s}} \times \mathbf{i} \Delta_\perp)}{2m} \\ &\quad \times S(-\Delta_\perp^2) e^{-i \Delta_\perp \cdot \mathbf{b}_\perp}. \end{aligned} \quad (61)$$

It is interesting to note that for a free elementary fermion, $\mathcal{E}^{(\text{asym})}(\mathbf{b}_\perp, \hat{\mathbf{b}}_\perp) = m \delta^{(2)}(\mathbf{b}_\perp)$ regardless of polarization; since $J_{\text{free}}(-\Delta_\perp^2) = S_{\text{free}}(-\Delta_\perp^2)$, the antisymmetric contribution to the energy density cancels the angular modulations that occurred in the symmetric EMT. Accordingly, for the asymmetric EMT, a synchronization-induced energy dipole moment arises from internal dynamics rather than being universally present in all fermions. The induced energy dipole moment in this case is

$$\mathbf{d}_E^{(\text{asym})} = \left(-\frac{1}{4} + \frac{1}{2} S(0) \right) \hat{e}_z \times \hat{\mathbf{s}} \approx -0.148 \hat{e}_z \times \hat{\mathbf{s}}, \quad (62)$$

if we use $S(0) = \frac{1}{2} (\Delta u^+ + \Delta d^+)$ from JAM estimates [81].

One benefit of the asymmetric EMT is that the energy and momentum *densities* are all trivial for a free elementary fermion, which appeals to intuition about the behavior of pointlike particles. The symmetric EMT, by contrast, suggests that pointlike fermions have nontrivial distributions of energy and momentum. To be sure, this picture seems more reasonable when recalling that fields are the fundamental objects of quantum field theories rather than particles; it is not farfetched to imagine that the fermion field can carry momentum around the center of an excitation in the field. For that matter, the flux densities in the asymmetric EMT of a free fermion are not zero, meaning that even the asymmetric EMT describes flows of energy and momentum—but flows that themselves contain zero momentum. In this regard, the symmetric EMT paints a more straightforward picture.

VI. CONCLUSIONS

In this work, we constructed and explored a formalism for obtaining exact, two-dimensional relativistic rest frame energy-momentum densities and currents for spin-zero and spin-half targets. We derived a general expression for these densities in terms of matrix elements of the EMT operator in Eq. (25), and subsequently obtained more explicit formulas for specific EMT components in terms of the

gravitational form factors. Additionally, we provided numerical estimates for what these densities may look like for a proton, using the holographic model of Mamo and Zahed [67,68] in light of the limited empirical data that exist.

The densities were obtained under a nonstandard time synchronization convention via tilted light front coordinates, which results in angular modulations in the densities of transversely polarized systems. These are similar to previously known modulations in the light front charge density [33,82], which arise at fixed light front time due to clock rate modulations for quarks moving toward or away from the observer. The energy density of transversely polarized targets has the peculiarity that its $\sin\phi$ modulations have the opposite sign from the modulations in any other density—in particular, energy bunches on the side of the target moving toward the observer rather than away. As discussed in Sec. V D, this is an artifact of the hadron's barycenter being the center of P_z rather than the center of energy. Curiously, the synchronization-induced energy dipole moment of a spin-half target is universally $-1/4$ if the symmetric Belinfante EMT is used to define the energy density—even for pointlike fermions. However, if the asymmetric EMT (defined by Leader and Lorcé [11]) is used instead, the energy dipole moment is nonuniversal and vanishes for pointlike fermions (see Sec. V F).

That the energy density should differ depending on whether the symmetric or asymmetric EMT is used may be the most peculiar and interesting of our results. It is not clear whether the energy density can be directly measured (as opposed to indirectly obtained by taking Fourier transforms of empirical gravitational form factors) so it is unclear that these cases can be empirically distinguished. Nonetheless, the energy density is one of the most preeminent desired quantities for describing hadron structure—being closely tied in with the mass decomposition and mass origin questions—and that the different EMT operators should entail different energy densities suggests that we ought to seriously consider which is more appropriate to use.

ACKNOWLEDGMENTS

We thank Ian Cloët, Wim Cosyn, Yang Li, Cédric Lorcé, and Andreas Metz for thought-provoking conversations that helped contribute to this work. This work was supported by the U.S. Department of Energy Office of Science, Office of Nuclear Physics under Award No. DE-FG02-97ER-41014. A. F. was additionally supported by the U.S. Department of Energy Contract No. DE-AC05-06OR23177, under which Jefferson Science Associates, LLC, operates Jefferson Lab. This work has been stimulated by the Quark Gluon Topical Collaboration of the U.S. Department of Energy.

APPENDIX A: BASIC IDENTITIES IN TILTED LIGHT FRONT COORDINATES

For convenience, we reproduce here several identities involving tilted light front coordinates from our previous work [33]. In this work, we do not use tildes to signify tilted coordinates, and expressions without explicit indication of the coordinate system should be assumed to be in tilted coordinates. By contrast, we explicitly signify instant form coordinates with a subscript or superscript IF.

Tilted light front coordinates are defined in terms of Minkowski (or instant form) coordinates as

$$\tau = x^0 \equiv t_{\text{IF}} + z_{\text{IF}}, \quad (\text{A1a})$$

$$x = x^1 \equiv x_{\text{IF}}, \quad (\text{A1b})$$

$$y = x^2 \equiv y_{\text{IF}}, \quad (\text{A1c})$$

$$z = x^3 \equiv z_{\text{IF}}. \quad (\text{A1d})$$

In this way, tilted coordinates operationally correspond to a change in the way that spatially distant clocks are synchronized [33,41,44,45]. The metric tensor and its inverse are

$$g_{\mu\nu} = \frac{\partial x_{\text{IF}}^\alpha}{\partial x^\mu} \frac{\partial x_{\text{IF}}^\beta}{\partial x^\nu} g_{\alpha\beta} = \begin{bmatrix} 1 & 0 & 0 & -1 \\ 0 & -1 & 0 & 0 \\ 0 & 0 & -1 & 0 \\ -1 & 0 & 0 & 0 \end{bmatrix}, \quad (\text{A2a})$$

$$g^{\mu\nu} = \frac{\partial x^\mu}{\partial x_{\text{IF}}^\alpha} \frac{\partial x^\nu}{\partial x_{\text{IF}}^\beta} g^{\alpha\beta} = \begin{bmatrix} 0 & 0 & 0 & -1 \\ 0 & -1 & 0 & 0 \\ 0 & 0 & -1 & 0 \\ -1 & 0 & 0 & -1 \end{bmatrix}. \quad (\text{A2b})$$

Covariant (lower-index) and contravariant (upper-index) four-vector components are related by

$$A_\mu = g_{\mu\nu} A^\nu, \quad A^\mu = g^{\mu\nu} A_\nu, \quad (\text{A3a})$$

which in terms of individual components gives

$$A_0 = A^0 - A^3, \quad A^0 = -A_3, \quad (\text{A3b})$$

$$A_1 = -A^1, \quad A^1 = -A_1, \quad (\text{A3c})$$

$$A_2 = -A^2, \quad A^2 = -A_2, \quad (\text{A3d})$$

$$A_3 = -A^0, \quad A^3 = -A_0 - A_3. \quad (\text{A3e})$$

The energy and momentum are defined to be time and space translation generators,

$$i[E, \hat{O}(x)] = \partial_0 \hat{O}(x), \quad (\text{A4a})$$

$$-i[\mathbf{p}, \hat{O}(x)] = \nabla \hat{O}(x), \quad (\text{A4b})$$

meaning they are related to covariant (lower-index) components of the four-momentum p_μ :

$$p_\mu \equiv (E; -p_x, -p_y, -p_z). \quad (\text{A5})$$

The tilted coordinate energy and momentum have the following relationships to instant form energy and momentum:

$$E = E^{\text{IF}}, \quad (\text{A6a})$$

$$p_x = p_x^{\text{IF}}, \quad (\text{A6b})$$

$$p_y = p_y^{\text{IF}}, \quad (\text{A6c})$$

$$p_z = E^{\text{IF}} + p_z^{\text{IF}}. \quad (\text{A6d})$$

The energy of a particle with mass m is given by

$$E = \frac{m^2 + \mathbf{p}^2}{2p_z}. \quad (\text{A7})$$

The momentum and velocity are related in the following way:

$$v_x = \frac{p_x}{p_z}, \quad (\text{A8a})$$

$$v_y = \frac{p_y}{p_z}, \quad (\text{A8b})$$

$$v_z = 1 - \frac{E}{p_z}. \quad (\text{A8c})$$

Notably, at rest, one has $\mathbf{p}_{\text{rest}} = (0, 0, m)$. This occurs because p_z is defined to be the generator of translations rather than to be proportional to velocity.

As usual, boosts transform contravariant four-vectors according to the formula

$$A'^\mu = \Lambda^\mu_\nu A^\nu. \quad (\text{A9})$$

An active transverse boost can be written in matrix form as

$$(\Lambda_\perp)^\mu_\nu = \begin{bmatrix} 1 & 0 & 0 & 0 \\ \beta_x & 1 & 0 & 0 \\ \beta_y & 0 & 1 & 0 \\ -\beta_\perp^2/2 & -\beta_x & -\beta_y & 1 \end{bmatrix}, \quad (\text{A10})$$

where $\boldsymbol{\beta}_\perp = (\beta_x, \beta_y)$ is the velocity of the boost. An active longitudinal boost can be written

$$(\Lambda_\parallel)^\mu_\nu = \begin{bmatrix} e^\eta & 0 & 0 & 0 \\ 0 & 1 & 0 & 0 \\ 0 & 0 & 1 & 0 \\ \sinh \eta & 0 & 0 & e^{-\eta} \end{bmatrix}. \quad (\text{A11})$$

Here, η is the rapidity of the longitudinal boost and is related to the velocity v_z of the boost by

$$\beta_z^\parallel = e^{-\eta} \sinh(\eta) = \frac{1}{2}(1 - e^{-2\eta}). \quad (\text{A12})$$

As discussed in the main text, we consider states with arbitrary momentum \mathbf{p} to be reached from the rest state through a longitudinal boost followed by a transverse boost. This combined boost can be written

$$(\Lambda)^\mu_\nu = (\Lambda_\perp \Lambda_\parallel)^\mu_\nu = \begin{bmatrix} e^\eta & 0 & 0 & 0 \\ e^\eta \beta_x & 1 & 0 & 0 \\ e^\eta \beta_y & 0 & 1 & 0 \\ e^\eta \beta_z & -\beta_x & -\beta_y & e^{-\eta} \end{bmatrix}. \quad (\text{A13})$$

Here,

$$\beta_z = e^{-\eta} \sinh(\eta) - \frac{\beta_\perp^2}{2} = \beta_z^\parallel - \frac{\beta_\perp^2}{2}, \quad (\text{A14})$$

as light front transverse boosts impart longitudinal velocity to the system, so the total longitudinal velocity of the combined boost differs from that of the longitudinal boost alone. Notably, the transverse boosts are defined to leave p_z invariant, but the relationship between p_z and v_z [see Eq. (A8)] means that v_z must change. From Eqs. (A7) and (A8), the boost that takes a system from rest to an arbitrary momentum \mathbf{p} can be written in terms of its energy and momentum as

$$\Lambda^\mu_\nu = \begin{bmatrix} p_z/m & 0 & 0 & 0 \\ p_x/m & 1 & 0 & 0 \\ p_y/m & 0 & 1 & 0 \\ (p_z - E)/m & -p_x/p_z & -p_y/p_z & m/p_z \end{bmatrix}. \quad (\text{A15})$$

APPENDIX B: PROOFS OF INTRINSIC DENSITY FORMULAS

In this appendix, we prove the intrinsic density formulas Eqs. (22) and (25). The premises underlying the proof are the universality (target independence) of the smearing functions in Eqs. (19) and (20), certain reasonable expectations for the intrinsic densities of point particles, and the

requirement that the smearing does not mix different irreducible representations of the Lorentz group.

Our strategy is to utilize the universality of the smearing functions. By finding the physical densities and the intrinsic densities in simple cases where both are already known, components of the smearing functions can be deduced. Since the smearing functions are target independent, these same smearing functions are also applicable to hadrons. We thus begin by proving Eqs. (21) and (24).

Once the smearing functions have been obtained, Eqs. (19) and (20) can be inverted to obtain general formulas for the intrinsic densities. Thus, after obtaining the smearing functions, we prove that Eqs. (22) and (25) are the results of this inversion.

Throughout this proof, we find it especially helpful to work with Fourier transforms, utilizing the convolution theorem. The Fourier transforms of Eqs. (19) and (20) are

$$\langle J^\mu(\Delta_\perp, \tau) \rangle_{2D} = \sum_{\lambda, \lambda'} \mathcal{P}^\mu_\nu(\Delta_\perp, \tau; \lambda, \lambda') j^\nu(\Delta_\perp; \lambda, \lambda') \Big|_{\Delta_z=0}, \quad (\text{B1a})$$

$$\langle T^{\mu\nu}(\Delta_\perp, \tau) \rangle_{2D} = \sum_{\lambda, \lambda'} \mathcal{Q}^{\mu\nu}_{\alpha\beta}(\Delta_\perp, \tau; \lambda, \lambda') t^{\alpha\beta}(\Delta_\perp; \lambda, \lambda') \Big|_{\Delta_z=0}, \quad (\text{B1b})$$

where Δ_\perp is the Fourier conjugate of the position argument. When these are written as functions of Δ_\perp , it should be implicitly assumed that we mean the Fourier transform of this function.

Given Eqs. (18) and (20), the Fourier transforms of the physical current and EMT densities can be written

$$\begin{aligned} \langle J^\mu(\Delta_\perp) \rangle_{2D} &= \sum_{\lambda, \lambda'} \int \frac{d^3\mathbf{P}}{2P_z(2\pi)^3} \langle \mathbf{p}, \lambda | \hat{\rho} | \mathbf{p}', \lambda' \rangle \\ &\times \frac{\langle \mathbf{p}', \lambda' | \hat{J}^\mu(0) | \mathbf{p}, \lambda \rangle}{2P_z} e^{i\Delta_0\tau} \Big|_{\Delta_z=0}, \end{aligned} \quad (\text{B2a})$$

$$\begin{aligned} \langle T^{\mu\nu}(\Delta_\perp) \rangle_{2D} &= \sum_{\lambda, \lambda'} \int \frac{d^3\mathbf{P}}{2P_z(2\pi)^3} \langle \mathbf{p}, \lambda | \hat{\rho} | \mathbf{p}', \lambda' \rangle \\ &\times \frac{\langle \mathbf{p}', \lambda' | \hat{T}^{\mu\nu}(0) | \mathbf{p}, \lambda \rangle}{2P_z} e^{i\Delta_0\tau} \Big|_{\Delta_z=0}, \end{aligned} \quad (\text{B2b})$$

where $\Delta_0 = p'_0 - p_0 = (\mathbf{P} \cdot \Delta_\perp) / P_z$. If we define non-script counterparts to the smearing functions via

$$\begin{aligned} \mathcal{P}^\mu_\nu(\Delta_\perp, \tau; \lambda, \lambda') &= \int \frac{d^3\mathbf{P}}{2P_z(2\pi)^3} \langle \mathbf{p}, \lambda | \hat{\rho} | \mathbf{p}', \lambda' \rangle \\ &\times \frac{m}{P_z} \mathbf{p}^\mu_\nu(\mathbf{P}, \Delta_\perp) e^{i\Delta_0\tau} \Big|_{\Delta_z=0}, \end{aligned} \quad (\text{B3a})$$

$$\begin{aligned} \mathcal{Q}^{\mu\nu}_{\alpha\beta}(\Delta_\perp, \tau; \lambda, \lambda') &= \int \frac{d^3\mathbf{P}}{2P_z(2\pi)^3} \langle \mathbf{p}, \lambda | \hat{\rho} | \mathbf{p}', \lambda' \rangle \\ &\times \frac{m}{P_z} \mathbf{q}^{\mu\nu}_{\alpha\beta}(\mathbf{P}, \Delta_\perp) e^{i\Delta_0\tau} \Big|_{\Delta_z=0}, \end{aligned} \quad (\text{B3b})$$

then Eq. (B1) can be reduced to

$$\frac{\langle \mathbf{p}', \lambda' | \hat{J}^\mu(0) | \mathbf{p}, \lambda \rangle}{2m} \Big|_{\Delta_z=0} = \mathbf{p}^\mu_\nu(\mathbf{P}, \Delta_\perp) j^\nu(\Delta_\perp; \lambda, \lambda'), \quad (\text{B4a})$$

$$\frac{\langle \mathbf{p}', \lambda' | \hat{T}^{\mu\nu}(0) | \mathbf{p}, \lambda \rangle}{2m} \Big|_{\Delta_z=0} = \mathbf{q}^{\mu\nu}_{\alpha\beta}(\mathbf{P}, \Delta_\perp) t^{\alpha\beta}(\Delta_\perp; \lambda, \lambda'). \quad (\text{B4b})$$

Thus Eq. (21) is true if $\mathbf{p}^\mu_\nu = \bar{\Lambda}^\mu_\nu$ and Eq. (24) is true if $\mathbf{q}^{\mu\nu}_{\alpha\beta} = (\bar{\Lambda}^\mu_\alpha \bar{\Lambda}^\nu_\beta - \frac{\Delta_\perp^2}{4P_z^2} \delta_3^\mu \delta_3^\nu \delta_\alpha^3 \delta_\beta^3)$. We shall proceed to prove these relations.

1. Constraints from Galilean densities

The components of the intrinsic densities with indices 0, 1, and 2 when written in contravariant form (i.e., with all indices raised) are known as Galilean densities [16,17], and we refer to them here as the Galilean components of j^μ and $t^{\mu\nu}$. The remaining non-Galilean components (those with a 3 as an index in contravariant form) do not mix into the Galilean components under transformations in the Galilean subgroup of the Poincaré group (see discussions in Refs. [16,33,36,83]). For these components, the intrinsic transverse densities are already known in the literature [16,17,27,33,36,37]. To obtain them, one simply applies the rest condition $\mathbf{P} = (0, 0, m)$ [see Eq. (A8)] to the kinematic components of the average target momentum in the standard hadronic matrix elements, and sets $\Delta_z = 0$ since the z coordinate is integrated out:

$$j^C(\Delta_\perp; \lambda, \lambda') = \frac{\langle \mathbf{p}', \lambda' | \hat{J}^C(0) | \mathbf{p}, \lambda \rangle}{2m} \Big|_{\mathbf{P}=(0,0,m), \Delta_z=0}, \quad (\text{B5a})$$

$$t^{CD}(\Delta_\perp; \lambda, \lambda') = \frac{\langle \mathbf{p}', \lambda' | \hat{T}^{CD}(0) | \mathbf{p}, \lambda \rangle}{2m} \Big|_{\mathbf{P}=(0,0,m), \Delta_z=0}. \quad (\text{B5b})$$

Here, we use uppercase Latin letters $\{A, B, C, D\}$ for indices constrained to $\{0, 1, 2\}$. On the other hand, the Galilean components of the left-hand side of Eq. (B4) are given by the same matrix elements without the rest condition applied. The matrix elements in the rest frame and moving frame are connected by Lorentz boosts, which in general require the application of Wigner rotations, as observed by Lorcé, for instance [38]. However, the spin dependence appearing in these matrix elements is through the light front helicity λ , which is invariant under light front boosts [33,83]. Thus, the Wigner rotations are trivial in this framework, and we simply have

$$\begin{aligned} & \langle \mathbf{p}', \lambda' | \hat{J}^A(0) | \mathbf{p}, \lambda \rangle_{\Delta_z=0} \\ & = \Lambda^A_C(\mathbf{P}) \langle \mathbf{p}', \lambda' | \hat{J}^C(0) | \mathbf{p}, \lambda \rangle_{\mathbf{P}=(0,0,m), \Delta_z=0}, \end{aligned} \quad (\text{B6a})$$

$$\begin{aligned} & \langle \mathbf{p}', \lambda' | \hat{T}^{AB}(0) | \mathbf{p}, \lambda \rangle_{\Delta_z=0} \\ & = \Lambda^A_C(\mathbf{P}) \Lambda^B_D(\mathbf{P}) \langle \mathbf{p}', \lambda' | \hat{T}^{CD}(0) | \mathbf{p}, \lambda \rangle_{\mathbf{P}=(0,0,m), \Delta_z=0}. \end{aligned} \quad (\text{B6b})$$

Crucially, the validity of these formulas follows from the fact that non-Galilean components do not mix into Galilean components under boosts; see Eq. (A15). Since for the Galilean components specifically, $\Lambda^A_C(\mathbf{P}) = \bar{\Lambda}^A_C$ [compare Eqs. (23) and (A15)], it follows that $\mathbf{p}^A_C = \bar{\Lambda}^A_C$ and $\mathbf{q}^{AB}_{CD} = \bar{\Lambda}^A_C \bar{\Lambda}^B_D$. Additionally, since we have seen that the Galilean components of the physical densities are independent of the non-Galilean components of the intrinsic densities, it follows that $\mathbf{p}^A_3 = 0$ and $\mathbf{q}^{AB}_{a3} = \mathbf{q}^{AB}_{3\beta} = 0$.

To deduce the remaining components of \mathbf{p} and \mathbf{q} , we consider pointlike targets. Since the smearing functions are universal (i.e., target independent), the smearing functions obtained for pointlike targets are also applicable to hadrons.

2. Remaining components of electromagnetic smearing function

The components \mathbf{p}^3_A for the electromagnetic smearing function can be deduced by considering a point particle with charge Q and magnetic dipole moment $\frac{\mu}{2m}$ in a definite-helicity state. The intrinsic Galilean charge and current densities are known, with the following Fourier transforms:

$$j^0(\Delta_\perp) = Q, \quad (\text{B7a})$$

$$\mathbf{j}_\perp(\Delta_\perp) = \frac{\mu\lambda}{2m} (\hat{e}_z \times \mathbf{i}\Delta_\perp). \quad (\text{B7b})$$

The matrix elements appearing in the physical densities are also known, and using identities in Appendix A of Ref. [33] gives

$$\begin{aligned} \frac{\langle \mathbf{p}', \lambda' | \hat{J}^\mu(0) | \mathbf{p}, \lambda \rangle}{2m} & = Q \frac{P^\mu}{m} + \frac{\mu\lambda}{2m} (\hat{e}_z \times \mathbf{i}\Delta_\perp)^\mu \\ & - \frac{\mu\lambda}{2m} (\hat{e}_z \times \mathbf{i}\Delta_\perp) \cdot \frac{\mathbf{P}}{P_z} \delta_3^\mu. \end{aligned} \quad (\text{B8})$$

From this and Eq. (23), a little algebra can be used to show

$$\frac{\langle \mathbf{p}', \lambda' | \hat{J}^\mu(0) | \mathbf{p}, \lambda \rangle}{2m} = \bar{\Lambda}^\mu_\nu j^\mu(\Delta_\perp). \quad (\text{B9})$$

Comparing to Eq. (B4), this shows that $\mathbf{p}^\mu_\nu = \bar{\Lambda}^\mu_\nu$ as long as $\mu \neq 3$ or $\nu \neq 3$; \mathbf{p}^3_3 remains undetermined because $j^3(\Delta_\perp) = 0$ in the case we just considered.

This last component can be obtained by considering the point charge to be polarized in the transverse plane. In this case, the charge density may (and, in fact, does) contain synchronization artifacts due to the presence of a z -direction current. However, the intrinsic current density of a point magnetic dipole is stationary and thus unaltered by synchronization effects. Accordingly, the intrinsic z -direction current has the Fourier transform

$$\mathbf{j}(\Delta_\perp) = \frac{\mu}{4m} \hat{s}_\perp \times \mathbf{i}\Delta_\perp. \quad (\text{B10})$$

Using identities from Appendix A of Ref. [33], the matrix element appearing in the physical four-current for this state is

$$\begin{aligned} \frac{\langle \mathbf{p}', \lambda' | \hat{J}^\mu(0) | \mathbf{p}, \lambda \rangle}{2m} & = \frac{P^\mu}{m} \left(Q + \frac{\mu}{2m} (\hat{s}_\perp \times \mathbf{i}\Delta_\perp) \cdot \hat{e}_z \right) \\ & + \frac{\mu}{4P_z} (\hat{s}_\perp \times \mathbf{i}\Delta_\perp)^\mu. \end{aligned} \quad (\text{B11})$$

One can read off the terms multiplying $\frac{P^\mu}{m}$ as coming from the intrinsic charge density. The remaining term is related to the intrinsic current density via

$$\begin{aligned} \frac{\mu}{4P_z} (\hat{s}_\perp \times \mathbf{i}\Delta_\perp)^3 & = \frac{m}{P_z} \frac{\mu}{4m} (\hat{s}_\perp \times \mathbf{i}\Delta_\perp)^3 \\ & = \bar{\Lambda}^3_3 j^3(\Delta_\perp), \end{aligned} \quad (\text{B12})$$

meaning $\mathbf{p}^3_3 = \bar{\Lambda}^3_3$. Thus $\mathbf{p}^\mu_\nu = \bar{\Lambda}^\mu_\nu$ holds for all components, from which Eq. (21) follows.

3. Remaining components of EMT smearing function

The remaining components of the EMT smearing function can be derived in a similar manner to the electromagnetic smearing functions, namely by considering pointlike particles. The universality of the smearing functions again means that the results are also applicable to hadrons.

As a first example, we consider a point mass without spin. The intrinsic EMT density of this system has a Fourier transform

$$t^{00}(\Delta_\perp) = m. \quad (\text{B13})$$

The matrix element appearing in the physical EMT density of the point mass (with zero D-term and no spin) is

$$\frac{\langle \mathbf{p}' | \hat{T}^{\mu\nu}(0) | \mathbf{p} \rangle}{2m} = m \frac{P^\mu P^\nu}{m^2} = \bar{\Lambda}^\mu_0 \bar{\Lambda}^\nu_0 t^{00}(\Delta_\perp). \quad (\text{B14})$$

Thus, $\mathbf{q}^{\mu\nu}_{00} = \bar{\Lambda}^\mu_0 \bar{\Lambda}^\nu_0$.

Next, we consider a point particle with spin oriented along the z axis. In addition to the intrinsic t^{00} density noted

above, there are additional momentum densities, with Fourier transforms

$$t^{0i}(\mathbf{\Delta}_\perp) = t^{i0}(\mathbf{\Delta}_\perp) = \frac{\lambda}{2}(\hat{e}_z \times i\mathbf{\Delta}_\perp)^i \quad (\text{B15})$$

for $i = 1, 2$, which reproduces a point distribution of total angular momentum $\lambda = \pm\frac{1}{2}$ at the origin. The matrix element appearing in the physical EMT density of this point particle is given by

$$\frac{\langle \mathbf{p}' | \hat{T}^{\mu\nu}(0) | \mathbf{p} \rangle}{2m} = m \left\{ \frac{P^\mu P^\nu}{m^2} + \frac{\lambda P^{\{\mu}(\hat{e}_z \times i\mathbf{\Delta}_\perp)^{\nu\}}}{m} - \frac{\lambda}{2}(\hat{e}_z \times i\mathbf{\Delta}_\perp) \cdot \frac{\mathbf{P}}{P_z} \frac{P^{\{\mu} \delta_3^{\nu\}}}{m} \right\}. \quad (\text{B16})$$

We already know the $\frac{P^\mu P^\nu}{m^2}$ structure is the contribution from the intrinsic t^{00} density. The new structure can be confirmed component by component to be equal to

$$\begin{aligned} & \frac{P^{\{\mu}(\hat{e}_z \times i\mathbf{\Delta}_\perp)^{\nu\}}}{m} - (\hat{e}_z \times i\mathbf{\Delta}_\perp) \cdot \frac{\mathbf{P}}{P_z} \frac{P^{\{\mu} \delta_3^{\nu\}}}{m} \\ &= \bar{\Lambda}^\mu_\alpha \bar{\Lambda}^\nu_\beta \bar{n}^{\{\alpha}(\hat{e}_z \times i\mathbf{\Delta}_\perp)^{\beta\}}, \end{aligned} \quad (\text{B17})$$

meaning that $\mathbf{q}^{\mu\nu}_{CD} = \bar{\Lambda}^\mu_C \bar{\Lambda}^\nu_D$, where $C, D \in \{0, 1, 2\}$. Components of \mathbf{q} with 3 in the latter two indices remain to be determined.

Just as with the electromagnetic case, we next consider a point mass with spin oriented in the transverse plane. The t^{00} density can (and will) obtain angular modulations, but the t^{03} and t^{30} densities—such as the j^3 density in the electromagnetic case—should be related to the longitudinally polarized t^{0i} densities by rotation, since the angular momentum is stationary. These Fourier transforms of densities are thus

$$t^{03}(\mathbf{\Delta}_\perp) = t^{30}(\mathbf{\Delta}_\perp) = \frac{\lambda}{2}(\hat{s} \times i\mathbf{\Delta}_\perp) \cdot \hat{e}_z. \quad (\text{B18})$$

The matrix element appearing in the corresponding physical EMT is

$$\frac{\langle \mathbf{p}' | \hat{T}^{\mu\nu}(0) | \mathbf{p} \rangle}{2m} = m \left\{ \frac{P^\mu P^\nu}{m^2} \left(1 + \frac{(\hat{s}_\perp \times i\mathbf{\Delta}_\perp) \cdot \hat{e}_z}{2m} \right) + \frac{\lambda P^{\{\mu}(\hat{s}_\perp \times i\mathbf{\Delta}_\perp)^{\nu\}}}{2P_z} \right\}. \quad (\text{B19})$$

The $\frac{P^\mu P^\nu}{m^2}$ piece (which indeed has angular modulations) can be read off as giving the intrinsic t^{00} density. For the remaining piece, one can confirm component by component that

$$\frac{P^{\{\mu}(\hat{s}_\perp \times i\mathbf{\Delta}_\perp)^{\nu\}}}{P_z} = \bar{\Lambda}^\mu_\alpha \bar{\Lambda}^\nu_\beta \bar{n}^{\{\alpha}(\hat{s} \times i\mathbf{\Delta}_\perp)^{\beta\}}, \quad (\text{B20})$$

from which it follows that $\mathbf{q}^{\mu\nu}_{C3} = \bar{\Lambda}^\mu_C \bar{\Lambda}^\nu_3$ and $\mathbf{q}^{\mu\nu}_{3D} = \bar{\Lambda}^\mu_3 \bar{\Lambda}^\nu_D$. Only \mathbf{q}^{33}_{33} remains undetermined.

The final component of the EMT smearing function is obtained by the requirement that different irreducible representations of the Lorentz group do not mix under smearing. The EMT operator can be decomposed into a pure trace part in the (0,0) representation and a traceless part in the (1,1) representation [3], and in principle the formalism considered in this work should be applicable to these parts separately.

A necessary condition for this requirement to be observed is that smearing maps the metric into itself:

$$\mathbf{q}^{\mu\nu}_{\alpha\beta} g^{\alpha\beta} = g^{\mu\nu}. \quad (\text{B21})$$

Using Eq. (23), and the equation for the tilted coordinate metric Eq. (A2), we find

$$\bar{\Lambda}^\mu_\alpha \bar{\Lambda}^\nu_\beta g^{\alpha\beta} = g^{\mu\nu} + \delta_3^\mu \delta_3^\nu \frac{\Delta_\perp^2}{4P_z^2}. \quad (\text{B22})$$

(This demonstrates that $\bar{\Lambda}$ is not a Lorentz boost, since Lorentz boosts leave the metric invariant.) Thus we observe that $\mathbf{q}^{\mu\nu}_{\alpha\beta} \neq \bar{\Lambda}^\mu_\alpha \bar{\Lambda}^\nu_\beta$ as has apparently been observed for all the other components, but that there must be a departure from this in order to preserve the metric. The metric is preserved if $\mathbf{q}^{33}_{33} = (\bar{\Lambda}^3_3 \bar{\Lambda}^3_3 - \frac{\Delta_\perp^2}{4P_z^2})$, which means that $\mathbf{q}^{\mu\nu}_{\alpha\beta} = (\bar{\Lambda}^\mu_\alpha \bar{\Lambda}^\nu_\beta - \frac{\Delta_\perp^2}{4P_z^2} \delta_3^\mu \delta_3^\nu \delta_\alpha^3 \delta_\beta^3)$. With this rule, the metric is preserved, and Eq. (24) follows.

4. Inversions of convolution formulas

Since we know that the smearing functions are given by Eqs. (21) and (24), the reduced convolution relations of Eq. (B4) can be written

$$\frac{\langle \mathbf{p}', \lambda' | \hat{J}^\mu(0) | \mathbf{p}, \lambda \rangle}{2m} = \bar{\Lambda}^\mu_\nu j^\nu(\mathbf{\Delta}_\perp; \lambda, \lambda'), \quad (\text{B23a})$$

$$\begin{aligned} \frac{\langle \mathbf{p}', \lambda' | \hat{T}^{\mu\nu}(0) | \mathbf{p}, \lambda \rangle}{2m} &= \left(\bar{\Lambda}^\mu_\alpha \bar{\Lambda}^\nu_\beta - \frac{\Delta_\perp^2}{4P_z^2} \delta_3^\mu \delta_3^\nu \delta_\alpha^3 \delta_\beta^3 \right) \\ &\times t^{\alpha\beta}(\mathbf{\Delta}_\perp; \lambda, \lambda'). \end{aligned} \quad (\text{B23b})$$

Since $\bar{\Lambda}$ is an invertible matrix (its determinant being 1), these equations can be inverted. For the current, this immediately gives Eq. (22). For the EMT, we have an additional step; matrix inversion gives

$$\begin{aligned} t^{\mu\nu}(\mathbf{\Delta}_\perp; \lambda, \lambda') &= \frac{\Delta_\perp^2}{4m^2} \delta_3^\mu \delta_3^\nu t^{33}(\mathbf{\Delta}_\perp; \lambda, \lambda') \\ &= \bar{\Lambda}^\mu_\alpha \bar{\Lambda}^\nu_\beta \frac{\langle \mathbf{p}', \lambda' | \hat{T}^{\alpha\beta}(0) | \mathbf{p}, \lambda \rangle}{2m}. \end{aligned} \quad (\text{B24})$$

For $\mu \neq 3$ or $\nu \neq 3$ the left-hand side is already the desired quantity $t^{\mu\nu}(\mathbf{\Delta}_\perp; \lambda, \lambda')$, while for $\mu = \nu = 3$ the equation needs to be divided by $(1 - \frac{\Delta_\perp^2}{4m^2})$ to obtain the desired quantity. From this, Eq. (25) follows. This completes the proof.

- [1] I. Yu. Kobzarev and L. B. Okun, Gravitational interaction of fermions, *Zh. Eksp. Teor. Fiz.* **43**, 1904 (1962).
- [2] Xiang-Dong Ji, A QCD analysis of the mass structure of the nucleon, *Phys. Rev. Lett.* **74**, 1071 (1995).
- [3] Xiang-Dong Ji, Breakup of hadron masses and energy—momentum tensor of QCD, *Phys. Rev. D* **52**, 271 (1995).
- [4] Cédric Lorcé, On the hadron mass decomposition, *Eur. Phys. J. C* **78**, 120 (2018).
- [5] Yoshitaka Hatta, Abha Rajan, and Kazuhiro Tanaka, Quark and gluon contributions to the QCD trace anomaly, *J. High Energy Phys.* **12** (2018) 008.
- [6] Andreas Metz, Barbara Pasquini, and Simone Rodini, Revisiting the proton mass decomposition, *Phys. Rev. D* **102**, 114042 (2021).
- [7] Xiangdong Ji, Proton mass decomposition: Naturalness and interpretations, *Front. Phys. (Beijing)* **16**, 64601 (2021).
- [8] Cédric Lorcé, Andreas Metz, Barbara Pasquini, and Simone Rodini, Energy-momentum tensor in QCD: Nucleon mass decomposition and mechanical equilibrium, *J. High Energy Phys.* **11** (2021) 121.
- [9] J. Ashman *et al.* (European Muon Collaboration), A measurement of the spin asymmetry and determination of the structure function $g(1)$ in deep inelastic muon-proton scattering, *Phys. Lett. B* **206**, 364 (1988).
- [10] Xiang-Dong Ji, Gauge-invariant decomposition of nucleon spin, *Phys. Rev. Lett.* **78**, 610 (1997).
- [11] E. Leader and C. Lorcé, The angular momentum controversy: What's it all about and does it matter?, *Phys. Rep.* **541**, 163 (2014).
- [12] Masashi Wakamatsu, Is gauge-invariant complete decomposition of the nucleon spin possible? *Int. J. Mod. Phys. A* **29**, 1430012 (2014).
- [13] Xiangdong Ji, Feng Yuan, and Yong Zhao, What we know and what we don't know about the proton spin after 30 years, *Nat. Rev. Phys.* **3**, 27 (2021).
- [14] M. V. Polyakov, Generalized parton distributions and strong forces inside nucleons and nuclei, *Phys. Lett. B* **555**, 57 (2003).
- [15] Maxim V. Polyakov and Peter Schweitzer, Forces inside hadrons: Pressure, surface tension, mechanical radius, and all that, *Int. J. Mod. Phys. A* **33**, 1830025 (2018).
- [16] Cédric Lorcé, Hervé Moutarde, and Arkadiusz P. Trawiński, Revisiting the mechanical properties of the nucleon, *Eur. Phys. J. C* **79**, 89 (2019).
- [17] Adam Freese and Gerald A. Miller, Forces within hadrons on the light front, *Phys. Rev. D* **103**, 094023 (2021).
- [18] Xiangdong Ji and Yizhuang Liu, Momentum-current gravitational multipoles of hadrons, *Phys. Rev. D* **106**, 034028 (2022).
- [19] Daniel Boer *et al.*, Gluons and the quark sea at high energies: Distributions, polarization, tomography, [arXiv: 1108.1713](https://arxiv.org/abs/1108.1713).
- [20] A. Accardi *et al.*, Electron Ion Collider: The Next QCD Frontier: Understanding the glue that binds us all, *Eur. Phys. J. A* **52**, 268 (2016).
- [21] R. Abdul Khalek *et al.*, Science requirements and detector concepts for the Electron-Ion Collider: EIC Yellow Report, *Nucl. Phys.* **A1026**, 122447 (2022).
- [22] Xiang-Dong Ji, Deeply virtual Compton scattering, *Phys. Rev. D* **55**, 7114 (1997).
- [23] A. V. Radyushkin, Nonforward parton distributions, *Phys. Rev. D* **56**, 5524 (1997).
- [24] A. V. Belitsky and A. V. Radyushkin, Unraveling hadron structure with generalized parton distributions, *Phys. Rep.* **418**, 1 (2005).
- [25] Gordon N. Fleming, *Charge distributions from relativistic form-factors*, in *Physical Reality and Mathematical Description: Festschrift Jauch (Josef Maria) on His 60th Birthday*, edited by Charles P. Enz and Jagdish Mehra (D. Reidel Publishing Company, Dordrecht, Holland, 1974), pp. 357–374.
- [26] Matthias Burkardt, Impact parameter dependent parton distributions and off forward parton distributions for $zeta \rightarrow 0$, *Phys. Rev. D* **62**, 071503 (2000); **66**, 119903(E) (2002).
- [27] Gerald A. Miller, Defining the proton radius: A unified treatment, *Phys. Rev. C* **99**, 035202 (2019).
- [28] E. Epelbaum, J. Gegelia, N. Lange, U. G. Meißner, and M. V. Polyakov, Definition of local spatial densities in hadrons, *Phys. Rev. Lett.* **129**, 012001 (2022).
- [29] Yang Li, Wen-bo Dong, Yi-liang Yin, Qun Wang, and James P. Vary, Minkowski's lost legacy and hadron electromagnetism, *Phys. Lett. B* **838**, 137676 (2023).
- [30] Yi Chen and Cédric Lorcé, Pion and nucleon relativistic electromagnetic four-current distributions, *Phys. Rev. D* **106**, 116024 (2022).
- [31] Adam Freese and Gerald A. Miller, Convolution formalism for defining densities of hadrons, *Phys. Rev. D* **108**, 034008 (2023).
- [32] J. Yu. Panteleeva, E. Epelbaum, J. Gegelia, and U. G. Meißner, Definition of gravitational local spatial densities for spin-0 and spin-1/2 systems, *Eur. Phys. J. C* **83**, 617 (2023).
- [33] Adam Freese and Gerald A. Miller, Light front synchronization and rest frame densities of the proton: Electromagnetic densities, *Phys. Rev. D* **107**, 074036 (2023).
- [34] Yi Chen and Cédric Lorcé, Nucleon relativistic polarization and magnetization distributions, *Phys. Rev. D* **107**, 096003 (2023).
- [35] J. Yu. Panteleeva, E. Epelbaum, J. Gegelia, and U. G. Meißner, Electromagnetic and gravitational local spatial densities for spin-1 systems, *J. High Energy Phys.* **07** (2023) 237.
- [36] Matthias Burkardt, Impact parameter space interpretation for generalized parton distributions, *Int. J. Mod. Phys. A* **18**, 173 (2003).
- [37] Gerald A. Miller, Transverse charge densities, *Annu. Rev. Nucl. Part. Sci.* **60**, 1 (2010).
- [38] Cédric Lorcé, Charge distributions of moving nucleons, *Phys. Rev. Lett.* **125**, 232002 (2020).
- [39] P. G. Blunden, M. Burkardt, and G. A. Miller, Light front nuclear physics: Toy models, static sources and tilted light front coordinates, *Phys. Rev. C* **61**, 025206 (2000).
- [40] Albert Einstein, On the electrodynamics of moving bodies, *Ann. Phys. (N.Y.)* **17**, 891 (1905).
- [41] H. Reichenbach, *The Philosophy of Space and Time*, Dover Books on Physics (Dover Publications, New York, 2012).
- [42] A. Grünbaum, *Philosophical Problems of Space and Time: Second, Enlarged Edition*, Boston Studies in the Philosophy and History of Science (Springer, Netherlands, 2012).

- [43] Yuan Zhong Zhang, Test theories of special relativity, *Gen. Relativ. Gravit.* **27**, 475 (1995).
- [44] Ronald Anderson, Geoffrey E. Stedman, and I. Vetharaniam, Conventionality of synchronisation, gauge dependence and test theories of relativity, *Phys. Rep.* **295**, 93 (1998).
- [45] Derek Muller and Petr Lebedev, Why No One Has Measured The Speed Of Light (2020), <https://www.youtube.com/watch?v=pTn6Ewhb27k>.
- [46] J. Yu. Panteleeva, E. Epelbaum, J. Gegelia, and U. G. Meißner, On the definition of electromagnetic local spatial densities for composite spin-1/2 systems, *Phys. Rev. D* **106**, 056019 (2022).
- [47] Adam Freese and Gerald A. Miller, Unified formalism for electromagnetic and gravitational probes: Densities, *Phys. Rev. D* **105**, 014003 (2022).
- [48] Taichiro Kugo and Izumi Ojima, Local covariant operator formalism of non-Abelian gauge theories and quark confinement problem, *Prog. Theor. Phys. Suppl.* **66**, 1 (1979).
- [49] F. J. Belinfante, On the spin angular momentum of mesons, *Physica (Amsterdam)* **6**, 887 (1939).
- [50] Adam Freese, Noether's theorems and the energy-momentum tensor in quantum gauge theories, *Phys. Rev. D* **106**, 125012 (2022).
- [51] Alexander L Fetter and John Dirk Walecka, *Theoretical Mechanics of Particles and Continua*, International Series in Pure and Applied Physics (McGraw-Hill, New York, NY, 1980).
- [52] C. K. Batchelor and G. K. Batchelor, *An Introduction to Fluid Dynamics*, Cambridge Mathematical Library (Cambridge University Press, Cambridge, England, 2000).
- [53] F. Irgens, *Continuum Mechanics* (Springer, Berlin Heidelberg, 2008).
- [54] John L. Friedman and Nikolaos Stergioulas, *Rotating Relativistic Stars*, Cambridge Monographs on Mathematical Physics (Cambridge University Press, Cambridge, England, 2013).
- [55] W. Flügge, *Tensor Analysis and Continuum Mechanics* (Springer Berlin Heidelberg, 2013).
- [56] I. S. Liu, *Continuum Mechanics*, Advanced Texts in Physics (Springer Berlin Heidelberg, 2013).
- [57] A. F. Bower, *Applied Mechanics of Solids* (Taylor & Francis Group, Boca Raton, FL, 2009).
- [58] J. L. Ericksen, Conservation laws for liquid crystals, *Trans. Soc. Rheol.* **5**, 23 (1961).
- [59] Dieter Forster, Tom C. Lubensky, Paul C. Martin, Jack Swift, and P. S. Pershan, Hydrodynamics of liquid crystals, *Phys. Rev. Lett.* **26**, 1016 (1971).
- [60] Helmut R. Brand and Harald Pleiner, Two-fluid model for the breakdown of flow alignment in nematic liquid crystals, *Phys. Rev. E* **103**, 012705 (2021).
- [61] John L. Friedman, James R. Ipser, and Subrahmanyan Chandrasekhar, Rapidly rotating relativistic stars, *Phil. Trans. R. Soc.* **340**, 391 (1992).
- [62] P. C. Martin, O. Parodi, and P. S. Pershan, Unified hydrodynamic theory for crystals, liquid crystals, and normal fluids, *Phys. Rev. A* **6**, 2401 (1972).
- [63] Adam Freese and Gerald A. Miller, Genuine empirical pressure within the proton, *Phys. Rev. D* **104**, 014024 (2021).
- [64] Cédric Lorcé, The relativistic center of mass in field theory with spin, *Eur. Phys. J. C* **78**, 785 (2018).
- [65] O. V. Teryaev, Spin structure of nucleon and equivalence principle, [arXiv:hep-ph/9904376](https://arxiv.org/abs/hep-ph/9904376).
- [66] Jonathan Hudson and Peter Schweitzer, Dynamic origins of fermionic D-terms, *Phys. Rev. D* **97**, 056003 (2018).
- [67] Kiminad A. Mamo and Ismail Zahed, Diffractive photo-production of J/ψ and Υ using holographic QCD: Gravitational form factors and GPD of gluons in the proton, *Phys. Rev. D* **101**, 086003 (2020).
- [68] Kiminad A. Mamo and Ismail Zahed, Nucleon mass radii and distribution: Holographic QCD, Lattice QCD and GlueX data, *Phys. Rev. D* **103**, 094010 (2021).
- [69] Mitsutoshi Fujita, Yoshitaka Hatta, Shigeki Sugimoto, and Takahiro Ueda, Nucleon D-term in holographic quantum chromodynamics, *Prog. Theor. Exp. Phys.* **2022**, 093B06 (2022).
- [70] J. J. Sakurai, Theory of strong interactions, *Ann. Phys. (N.Y.)* **11**, 1 (1960).
- [71] T. H. Bauer, R. D. Spital, D. R. Yennie, and F. M. Pipkin, The hadronic properties of the photon in high-energy interactions, *Rev. Mod. Phys.* **50**, 261 (1978); **51**, 407(E) (1979).
- [72] Koji Hashimoto, Tadakatsu Sakai, and Shigeki Sugimoto, Holographic baryons: Static properties and form factors from gauge/string duality, *Prog. Theor. Phys.* **120**, 1093 (2008).
- [73] P. E. Shanahan and W. Detmold, Gluon gravitational form factors of the nucleon and the pion from lattice QCD, *Phys. Rev. D* **99**, 014511 (2019).
- [74] B. Duran *et al.*, Determining the gluonic gravitational form factors of the proton, *Nature (London)* **615**, 813 (2023).
- [75] Pere Masjuan, Enrique Ruiz Arriola, and Wojciech Broniowski, Meson dominance of hadron form factors and large- N_c phenomenology, *Phys. Rev. D* **87**, 014005 (2013).
- [76] DLMF, *NIST Digital Library of Mathematical Functions*, edited by f. W. J. Olver, A. B. Olde Daalhuis, D. W. Lozier, B. I. Schneider, R. F. Boisvert, C. W. Clark, B. R. Miller, B. V. Saunders, H. S. Cohl, and M. A. McClain, <http://dlmf.nist.gov/>, Release 1.1.0 of 2020-12-15.
- [77] Gerald A. Miller, Singular charge density at the center of the pion?, *Phys. Rev. C* **79**, 055204 (2009).
- [78] Julia Yu. Panteleeva and Maxim V. Polyakov, Forces inside the nucleon on the light front from 3D Breit frame force distributions: Abel tomography case, *Phys. Rev. D* **104**, 014008 (2021).
- [79] Brandon Kriesten, Simonetta Liuti, Liliet Calero-Diaz, Dustin Keller, Andrew Meyer, Gary R. Goldstein, and J. Osvaldo Gonzalez-Hernandez, Extraction of generalized parton distribution observables from deeply virtual electron proton scattering experiments, *Phys. Rev. D* **101**, 054021 (2020).
- [80] Jian-Wei Qiu and Zhite Yu, Single diffractive hard exclusive processes for the study of generalized parton distributions, *Phys. Rev. D* **107**, 014007 (2023).
- [81] C. Cocuzza, W. Melnitchouk, A. Metz, and N. Sato (Jefferson Lab Angular Momentum (JAM) Collaboration),

Polarized antimatter in the proton from a global QCD analysis, [Phys. Rev. D **106**, L031502 \(2022\)](#).

- [82] Carl E. Carlson and Marc Vanderhaeghen, Empirical transverse charge densities in the nucleon and the nucleon-to-Delta transition, [Phys. Rev. Lett. **100**, 032004 \(2008\)](#).
- [83] D. E. Soper, Infinite-momentum helicity states, [Phys. Rev. D **5**, 1956 \(1972\)](#).